1 **Arctic Ocean outflow and glacier-ocean interaction modify water over the Wandel Sea shelf**

2 **(Northeast Greenland)**

5 Igor A. Dmitrenko[1]*, Sergey A. Kirillov[1], Bert Rudels[2], David G. Babb[1], Leif Toudal Pedersen[3], Søren

6 Rysgaard[1,4,5], Yngve Kristoffersen[6,7] and David G. Barber[1]

9 [1]Centre for Earth Observation Science, University of Manitoba, Winnipeg, Canada

10 [2]Finnish Meteorological Institute, Helsinki, Finland

11 [3] Technical University of Denmark, Lyngby, Denmark

12 [4]Greenland Climate Research Centre, Greenland Institute of Natural Resources, Nuuk, Greenland

13 [5]Arctic Research Centre, Aarhus University, Aarhus, Denmark

14 [6]Department of Earth Science, University of Bergen, Bergen, Norway

15 [7] Nansen Environmental and Remote Sensing Centre, Bergen, Norway

22 *Corresponding author, e-mail: igor.dmitrenko@umanitoba.ca

Abstract: The first-ever conductivity-temperature-depth (CTD) observations on the Wandel Sea shelf in North Eastern Greenland were collected in April-May 2015. They were complemented by CTDs taken along the continental slope during the Norwegian FRAM 2014-15 drift. The CTD profiles are used to reveal the origin of water masses and interactions with ambient water from the continental slope and the tidewater glacier outlet. The subsurface water is associated with the Pacific Water outflow from the Arctic Ocean. The underlying Halocline separates the Pacific Water from a deeper layer of Polar Water that has interacted with the warm Atlantic water outflow through Fram Strait recorded below 140 m. Over the outer shelf, the Halocline shows numerous cold density-compensated intrusions indicating lateral interaction with an ambient Polar Water mass across the continental slope. At the front of the tidewater glacier outlet, colder and turbid water intrusions were observed at the base of the Halocline. On the temperature-salinity plots these stations indicate a mixing line that is different from the ambient water and seems to be conditioned by the ocean-glacier interaction. Our observations of Pacific Water are set within the context of upstream observations in the Beaufort Sea and downstream observations from the Northeast Water Polynya, and clearly show the modification of Pacific water during its advection across the Arctic Ocean. Moreover, ambient water over the Wandel Sea slope shows different thermohaline structures indicating the different origin and pathways of the on-shore and off-shore branches of the Arctic Ocean outflow through western Fram Strait.

1. Introduction

One of the most significant global issues over the last decade has been the vast change in the Arctic region. The Arctic Science Partnership (ASP) consortium (www.asp-net.org) was established to understand connections and processes linking climate, cryosphere, ocean and ecosystems. Under the framework of ASP, an extensive oceanographic field campaign took place during April and May 2015 from the landfast sea ice that covers the shelf of the Wandel Sea.

47   The field campaign was based out of the new Villum Research Station located at the Danish

48   military outpost Station Nord at 81°36N, 16°40W on Prinsesse Ingeborg Peninsula in the very north-

49   eastern corner of Greenland (Figures 1 and 2). Northern Greenland is among the most remote wildernesses

50   of the northern hemisphere. Station Nord features a very cold polar tundra climate with an average

51   temperature during winter below -30°C and just a few degrees above the freezing point in the midst of the

52   short summer.

53   The Wandel Sea is predominantly covered by landfast multiyear sea ice all year around, and only

54   the interior of fjords may become ice free during late summer (Figure 2b). The Flade Isblink Ice Cap is

55   located close to Station Nord (Figures 2b and 3). It is an isolated ice cap with a surface area of 5 000 km^2

56   and maximum thickness of 600 m that overlies bedrock that is on average 100 m below sea level [e.g.,

57   *Palmer et al*., 2010; *Rinne et al*., 2011]. In general, the Wandel Sea is rather a glacial inlet than a shelf sea.

58   It is comprised by several fjords open to the continental slope (Figure 2b). The landfast ice edge in Figure

59   2b roughly marks the Wandel Sea continental shelf break located in about 35-45 km from the fjord mouths.

60   The bathymetry of the Wandel Sea shelf and upper continental slope is poorly known. *Nørgaard-Pedersen*

61   *et al*. [2008] provided limited information on the bottom topography in the area surrounding Station Nord,

62   specifically the existence of several submarine glacial troughs, with depths of up to ~180 m, that open to

63   the continental slope (Figure 4a). The bathymetry of the Independence and Denmark fjords is unknown.

64   Prior to our field program in 2015, there were no oceanographic or in situ sea ice observations over

65   the Wandel Sea shelf. From very general considerations, the Wandel Sea shelf is expected to be under the

66   influence of the Arctic Ocean outflow through western Fram Strait (Figure 1). The upper layer (down to

67   400 m) of this outflow is comprised of low salinity surface Polar Water partly including low salinity water

68   of Pacific origin, and the intermediate water (> 150-200 m) of Atlantic origin [e.g., *Rudels et al*., 2002;

69   2005]. The freshwater export through western Fram Strait is an important component of the Arctic Ocean

70   freshwater budget that links the Arctic Ocean to the global climate system [e.g., *de Steur et al*., 2009]. The

71   coastal branch of the Pacific water flow along the southeast coast of Greenland was reported based on

72 observations [e.g., *Bacon et al.*, 2002; *Sutherland and Pickart*, 2008; *Sutherland et al.* 2009] and

73 numerical simulations [*Hu and Myers*, 2013; *Aksenov et al.*, 2016]. However, the pathways of the low

74 salinity Pacific water along the northeast coast of Greenland are debatable. The Wandel Sea shelf can also

75 be a source of freshwater that originates from summer snow/sea ice meltwater and from glacier-derived

76 freshwater.

77   The Atlantic Water outflow through Western Fram Strait with temperatures above 0°C in the

78 intermediate water layer (> 150-200 m) closes the circulation loop of the Atlantic Water in the Arctic

79 Ocean conditioned by its inflow through eastern Fram Strait and Barents Sea [e.g., *Rudels et al., 1994*;

80 *Rudels*, 2012] – Figure 1. The interaction of warm Atlantic Water with tidewater glacier outlets along the

81 southeast coast of Greenland results in ocean-driven glacier melting. This generates additional fresh water

82 flux contributing to the regional fresh water budget [e.g., *Straneo et al.*, 2011, 2012; *Sutherland and*

83 *Straneo*, 2012; *Inall et al.*, 2014]. For the Wandel Sea shelf, the efficiency of the glacier-ocean interaction

84 is not assessed because of the unknown oceanographic conditions at the glacier-ocean interface.

85   This paper is focused on analysis of the first-ever conductivity-temperature-depth (CTD)

86 observations on the Wandel Sea shelf collected from the landfast ice in April-May 2015 (Figure 3) to put

87 this region in the context of upstream, downstream and local conditions with a special focus on the Arctic

88 Ocean outflow and ocean-glacier interaction This data set was complemented by CTDs taken in June-July

89 2015 over the Wandel Sea continental slope during the Norwegian FRAM 2014-15 sea ice drift (Figure

90 2b). Our objectives were to investigate the principal features of vertical profiles of salinity and temperature

91 taken over the shelf regions deeper than 100 m for tracing the water origin and local modifications.

92   The paper is structured as follows. Section 2 describes observational data on CTD, sea-ice and

93 bottom topography, and justifies the selection of CTD data for our analysis. Section 3 provides detailed

94 description of the water mass structure over the Wandel Sea shelf and continental slope, methods of

95 clustering the CTD profiles and the CTD clusters. Section 4.1 discusses oceanographic patterns of the

96 "glacier" CTD cluster with respect to the ocean-glacier interaction. Section 4.2 focuses on the "intrusive"

97 CTD cluster from the Wandel Sea outer shelf. Sections 4.3/4.4 discuss local/remote origins of the Wandel

98 Sea water masses. Finally, section 5 concludes the analysis and discusses limitations.

99

100 **2. Data and methods**

101 Between 17 April and 15 May 2015, 86 CTD profiles (labelled SN15 − XX; XX is the station

102 number) were collected from the landfast sea ice (1.0 to 3.5 m thick) on the Wandel Sea shelf in Northeast

103 Greenland (Figures3 and 4). The CTD observations were carried out with a SBE-19plus CTD that was

104 calibrated prior to the expedition, and was accurate to ±0.005°C and ±0.0005 S/m. The CTD was outfitted

105 with a Seapoint Turbidity Meter that measured turbidity in nephelometric turbidity units (NTU).

106 Additionally we used vertical profiles of the colored dissolved organic matter (CDOM) from an Ice

107 Tethered Profiler (ITP) by McLane Research Laboratory that was temporarily deployed at SN15-13 from

108 21 April to 11 May. The ITP collected a profile every 2 hours between 3 m and 101 m depth, and was

109 equipped with a Wetlabs ECO sensor for measuring backscatter intensity, Chlorophyll fluorescence and

110 CDOM fluorescence for EX/EM = 370/460 nm. CDOM data was recorded approximately every 1.5 m with

111 sensitivity of 0.28 parts per billion (ppb). Other ITP data from this temporary deployment are not used

112 within this paper.

113 Four sets of complementary CTD profiles are used to provide context for the water masses we

114 observed over the Wandel Sea shelf. CTD profiles collected in the Beaufort Sea between 225°E and 226°E

115 between June and October from 2002 to 2011 by ArcticNet (Figure 1) were averaged and reveal the mean

116 summer water profile in the Beaufort Sea, which we consider the 'upstream' area. CTD profiles collected

117 over the Wandel Sea continental slope during June and July 2015 from the research hovercraft

118 SABVABAA during the Norwegian FRAM 2014/15 sea ice drift (Figure 2b) are used to represent the

119 ambient water masses and compared against a CTD profile collected in August 2008 from the RV

120   *Polarstern* [*Kattner*, 2009]. Furthermore we adopted a CTD profile taken in a rift in the 79 North Glacier

121   in August 2009 – Figure 2b [*Straneo et al.*, 2012].

122   Ice conditions over the Wandel Sea shelf, the adjoining fjords and the Greenland Sea continental

123   slope were monitored by MODIS (Moderate Resolution Imaging Spectroradiometer – Figure 2b) and

124   Sentinel-1 C- band SAR (C-Band Synthetic Aperture Radar – Figure 3) satellite imagery, acquired daily by

125   the Danish Meteorological Institute (http://ocean.dmi.dk/arctic/nord.uk.php). In general, newly formed sea-

126   ice, ice ridges, multiyear and first-year landfast sea ice, refrozen leads, large icebergs and glacier

127   terminations are distinguishable in SAR imagery. Sea ice thickness was measured manually at each CTD

128   station with an ice thickness tape.

129   Within this study we are interested in resolving the vertical thermohaline structure below the

130   freshened surface waters, including the water layer below the lower boundary of the glacier tongue (>~90

131   m depth) and a warmer Atlantic-derived water layer with temperature > 0°C below ~140 m depth.

132   Therefore we only use the 31 CTD profiles that were performed in waters deeper than 100 m (Figure 4).

133   Over the Wandel Sea shelf there are three regions with depths greater than 100 m. These regions are

134   separated laterally by ~20-30 m deep shoals, but are likely connected to submarine troughs that lead

135   towards the continental slope [*Nørgaard-Pedersen et al.*, 2008].

136   The primary region with depth exceeding 100 m is located over a submarine glacial trough to the

137   north-northeast of Station Nord that ranges in depth from 110-130 m at the tidewater glacier outlet

138   (STN15-13 and 75) to 183 m further off-shore along the trough (STN15-63; Figure 4). The glacial trough

139   has been formed by the Flade Isblink Ice Cap [e.g., *Palmer et al.*, 2010; *Rinne et al.*, 2011]. During our

140   surveys this area was predominantly covered by landfast multiyear sea ice (~3.5 m thick; lighter colours in

141   Figure 3). Several CTD stations were performed through refrozen leads that contained younger and

142   therefore thinner sea ice (~1.5 m thick; darker colours in Figure 3). The glacial trough was paralleled on

143   both sides by numerous icebergs that appeared to be grounded on the marginal lateral moraine which can

144   significantly suppress lateral exchange with ambient water from the continental slope (Figure 3). However,

145 lateral exchange still might be possible given the narrow glacial troughs that exist across these shallow

146 shoals [*Nørgaard-Pedersen et al.*, 2008].

147 Another area with depth exceeding 100 m is located to the northwest of Station Nord between

148 Prinsesse Thyra and Prinsesse Margreth Islands with depths of 104/112 m (stations STN15-53/54; Figure

149 4). The region was covered by ~1.2 m of sea ice that grew within a refrozen lead after it opened in August

150 2012 (Figure 3). We speculate that the gradual increase in depth along the CTD transect that ended at

151 STN15-54 continues out along the trough towards the continental slope; however, no bathymetric data is

152 available beyond STN15-54.

153 The glacial trough to the west-southwest of Station Nord from the glacial outlet of the Flade Isblink

154 ice cap to the west of Prinsesse Dagmar Island also exceeds 100 m depth (Figure 4a). During our field work

155 the glacier was grounded at ~35-40 m depth. The trough extending from this outlet glacier quickly reached

156 depths of ~100 m (STN15-35) and reached a maximum depth of 127 m (STN15-79). During the field

157 campaign this region was covered with a mix of first year (~1.2 m thick) and multiyear sea ice (~3 m

158 thick), with icebergs and an ice island frozen within the fast ice (Figure 3) that corresponds to the typical

159 ice conditions over this area. During August 2014 (Figure 2) as well as during August 2010-2012 this

160 region was ice-free (http://ocean.dmi.dk/arctic/nord.uk.php).

161

162 **3. Results**

163 **3.1. Water mass structure**

164 The water column over the Wandel Sea shelf shows six distinct layers (Figure 5). The layer

165 immediately below the ice (~1.5–5 m) was relatively fresh (salinity of 16-21; Figure 5) as a result of

166 summer snow/sea ice melt water and freshwater from the glacial runoff [*Bendtsen et al.*, 2017]. Several

167 stations had extremely fresh surface waters (salinity of 1-12; Figure 5) that appeared to be part of under-ice

168 ponds [e.g. *Eicken,* 1994; *Flocco et al.,* 2015] comprised of melt water trapped in pockets below the

169 multiyear landfast ice. This surface layer freshened during the melt season and was observed to have

170 salinities of 1-8 during CTD transects in August 2015 [*Bendtsen et al.,* 2017]. The sub-surface halocline

171 layer is characterised by a strong vertical salinity gradient (salinity 1 m^{-1}) down to 15 m depth (Figure 5).

172 The sub-surface halocline separated the fresh surface waters from a layer with weak vertical salinity

173 gradients (salinity 30 to 31.2) and water near the freezing point (blue dashed line Figure 5) that reached to

174 ~65 m depth (Figure 5). *Shimada et al.,* [2005] identified this layer in the Canada Basin and referred to it as

175 a "cold halostad", thus over the Wandel Sea shelf we refer to this layer as the "Halostad" (Figure 5, Table

176 1).

177   Below the Halostad (below 75 m depth), temperatures increased steadily through the Halocline

178 (with salinity centered around 33) and Atlantic modified Polar Water (PrW) – Figure 5 and Table 1. The

179 Halocline is further distinguished from the Halostad and PrW by its high vertical salinity gradient of 0.07

180 m^{-1} (Figure 5). Temperatures eventually exceeded 0°C (the commonly accepted upper boundary of the

181 Atlantic layer) at ~140 m depth indicating the presence of Atlantic Water (AW) below this depth (Table 1).

182 Atlantic modification of the Halocline is evident from the increase in temperature through the Halocline.

183 Furthermore, the Halocline shows intrusions of cooler water, which is further described and discussed for

184 tracing the shelf-slope and ocean-glacier interactions, as well as the Pacific Water (PcW) and AW outflow

185 from the Arctic Ocean through western Fram Strait.

186   Comparing CTD profiles collected over the Wandel Sea shelf (solid lines) and those collected off-

187 shelf (dashed lines) reveals substantial differences in the temperature profiles down to 180 m, and in the

188 salinity profiles down to 110 m (Figure 5). In 2015, the Halostad and Halocline over the Wandel Sea shelf

189 were not observed over the continental slope (Figure 5). Moreover, the thermocline was typically 20-30 m

190 deeper off the shelf (red dashed lines Figure 5), specifically the upper boundary of the AW was found at

191 170 m compared to 140 m on the shelf. We also present a CTD profile collected on the upper continental

192 slope in 2008 (dot lines in Figure 5), which reveal little variability in the water mass structure between

193 2008 and 2015 and indicate that the off-shelf water mass structure is characterized by a colder, thicker and

194 more saline Halostad that is derived from the Lower Halocline in the Nansen Basin [*Rudels et al.*, 1996].

195 We note, however, that the synoptic, seasonal and interannual variability can be significant [e.g., *Falck et*

196 *al.*, 2005] making it difficult to interpret the snapshot data from the Wandel Sea continental slope, while

197 this analysis appears important and plausible

198

199 **3.2. CTD clustering**

200 **3.2.1. *Methods of CTD clustering***

201 In the following, we focus on the water layer below the sub-surface Halocline, comprised of the

202 Halostad, Halocline, PrW and AW layers (Figures 5-7, Table 1). The 31 CTD profiles with depths greater

203 than 100 m were subdivided into clusters according to their temperature-salinity (*TS*) curves and their

204 variability in the *TS* space (Figures 4b, 6 and 7 and Table 2). The clustering was conducted to assess the

205 origin of water masses, and to identify the shelf-slope and ocean-glacier interactions. For clustering we use

206 the following criteria. (i) For the salinity range $30 < S < 31.2$ (~15-65 m depth; Halostad; gray shaded area

207 Figure 6) we differentiate profiles based on their proximity to the freezing temperature (blue dashed line

208 Figure 6), which indicates how the water thermal properties have been modified. (ii) For the salinity range

209 $31.2 < S < 33.5$ (~65-90 m depth; upper Halocline; green shaded area Figures 6 and 7) we differentiate

210 clusters based on the appearance of distinctive thermohaline intrusions within the TS curves. These

211 intrusions increase the TS variability and disrupt the initially smooth TS curves, which indicate interaction

212 between ambient water masses. These features have been used to trace the origin and pathways of water

213 masses in the Arctic Ocean [e.g., *Walsh and Carmack*, 2003; *Rudels et al.*, 1994; 2005; *Woodgate et al.*,

214 2007] and identify shelf-glacier interactions [*Jenkins*, 1999; *Stevens et al.*, 2016]. (iii) For the salinity range

215 > 33.5 (> 90 m depth; low Halocline; pink shaded area; Figures 6 and 7) we use the appearance of

216 thermohaline intrusions and the slope of the mixing line to differentiate the clusters (Figures 7d and 7e).

217 The displacement of the mixing line indicates the thermodynamic "meltwater" end member [e.g., *Jenkins*,

218 1999; *Straneo et al.*, 2012; *Wilson and Straneo*, 2015].

219   The intrusions along isohalines suggest isopycnal interleaving occurs within the area (Figures 6b

220   and 7c). Thus, one along-isopycnal standard deviation of the mean temperature and salinity was employed

221   to estimate the efficiency of intrusive activity for every 0.1 kg m^{-3} interval of the potential density. All TS

222   curves exceeding ±1 standard deviation at more than 50% of the 0.1 kg m^{-3} intervals were added to the

223   different clusters based on the prescribed salinity range. We also defined a "transit" cluster (Figure 7b)

224   showing weak thermohaline intrusions below one standard deviation of the mean.

225   Based on our criteria, all CTD profiles ≥ 100 m depth were subdivided into five clusters (Table 2

226   and Figures 4b, 6 and 7).

227

228   **3.2.2. *Description of clusters***

229   Here we assess the main patterns of clusters putting them in the context of their geographical

230   location on the Wandel Sea shelf and the sea-ice features.

231   Cluster I is comprised of the nine CTD stations occupied (i) along the glacial trough to the west-

232   southwest of Station Nord and (ii) between Prinsesse Thyra and Prinsesse Margreth Islands (SN15-

233   31/35/53/54/79-83; Figures 4b and 6a). This cluster is distinguished by two features: (i) a relatively warm

234   Halostad overlying the Halocline above 65 m (30 < S < 31.2) and (ii) smooth *TS* curves through the

235   underlying water column (S > 31.2) that appear to be unaffected by intrusive activity (Figure 6a). The

236   highest temperature offset from the potential freezing temperature is associated with CTD profiles from the

237   glacial trough, which was ice-free during the preceding summer (Figure 2b) and therefore warmed through

238   solar heating. Region between islands was most recently ice-free during August 2013 (not shown), which

239   likely led to the creation of a relatively warm subsurface layer. Thus, we subsequently refer to Cluster I as

240   the "open water" cluster.

241   Cluster II (6 stations: SN15-8-11/66/68; Figures 4b, 6b and 7a) is characterised by smooth *TS*

242   curves slightly affected by intrusive activity (Figure 7a), with water near the potential freezing temperature

243   in the Halostad (S < 31.2; gray shading in Figure 6b). Stations from this cluster occupy the middle of the

244 glacial trough to the north of Station Nord and were covered by multiyear landfast ice during our field

245 program. In the following we assume that Cluster II represents the background oceanographic conditions

246 over the Wandel Sea shelf, and subsequently refer to this group as the "basic" cluster.

247   Cluster III (6 stations: SN15-6/7/58/59/67/71; Figures 4b, 6b and 7b) is characterized by

248 temperatures that remain within 1 standard deviation through salinities between 31.2 and 33.5 (green

249 shaded area, Figures 6b and 7b), except for two profiles that deviate from the mean by -0.1 to -0.2°C along

250 the 26.9±0.1 kg m^{-3} isopycnal. In general, stations from Cluster III occupy almost the same area as Cluster

251 II (Figure 4b) and represent the transition from Cluster II, with smooth *TS* curves, to Cluster IV, strongly

252 impacted by intrusive activity. Thus, we refer to this cluster as the "transit" cluster.

253   Cluster IV (6 stations: SN15-62-65/69/70; Figures 4b, 6b and 7c) profiles display the most

254 significant intrusive activity within the Halocline between salinities of 31.2 and 33.5 (Figures 6b and 7c).

255 Within this range all *TS* curves show negative temperature anomalies greater than one standard deviation

256 for at least half of the 0.1 kg m^{-3} intervals (Figure 7c). In contrast, the profiles from this cluster have

257 positive temperature anomalies of about one standard deviation throughout the underlying water where $S >$

258 33.5. Profiles from this cluster were taken over the compact area on the eastern flank of the glacial trough

259 on the Wandel Sea outer shelf (Figure 4b) and are the closest profiles to the continental slope. Hereafter we

260 refer to these stations as the "intrusive" cluster.

261   Cluster V (4 stations: SN15-13/72/73/75; Figures 4b, 6b and 7d) is characterized by profiles that (i)

262 show exceptionally strong intrusive activity in the *TS* plot for $33.5 < S < 33.85$ (90-100 m depth) and (ii)

263 comprise a new mixing line for the underlying water layer ($S > 33.85$, >100 m depth) which is remarkably

264 different from the ambient Clusters II-IV (Figures 7d and 7e). For stations SN15-13/72/75, thermohaline

265 intrusions show density-compensated negative salinity/temperature anomalies of up to -0.03/-0.32°C, and

266 exceed the mean by more than two standard deviations. Station SN15-73 shows smaller intrusions, but they

267 still exceed the mean by about one standard deviation. For $S > 33.9$, profiles from this cluster align with a

268   distinct mixing line that is shifted towards lower temperatures relative to the ambient profiles. Profiles

269   from this cluster were collected near the front of the glacial tongue, thus we refer to this cluster as the

270   "glacier" cluster.

271

272   **4. Discussion**

273   Below we discuss the potential origin and modifications of the water masses in clusters II, IV and V

274   we have identified over the Wandel Sea shelf. We also use our findings to trace the Arctic Ocean outflow

275   through western Fram Strait, putting our results into the context of upstream observations in the Canada

276   Basin and downstream observations in the Northeast Water Polynya (NEW).

277

278   **4.1. Shelf water interaction with tidewater glacier**

279   We speculate that cluster V shows features that we attribute to the ocean-glacier interaction. These

280   are (i) the abnormal intrusive activity at the base of the Halocline and (ii) the transition of profiles in the *TS*

281   space towards a new mixing line for the underlying Atlantic modified PrW at the glacier front (Figures 7d

282   and 7e). The ambient water from Clusters II-IV exhibits a background mixing line between the Halocline

283   and AW (Figure 6b) which seems to be unaffected by the ocean-glacier interaction. During summer,

284   significant surface glacial runoff provides a new end-member to this mixture. However, during winter there

285   is no surface glacial runoff, and subglacial runoff is negligible, as confirmed by our CTD profiles during

286   April and May that show no surface salinity gradient around the termination of the glacier. Even though

287   glacial melt water is negligible during winter, the glacier can still modify the ambient mixing line through

288   ocean-glacier interactions as we will discuss below.

289   Water cools when it comes in contact with glacier ice that is colder than the *in situ* freezing point.

290   For example, for the Ross Ice Shelf in Antarctica, *Wexler* [1960] reported the glacier ice temperature

291   increased from -22°C at the surface to -14°C at 200 m depth and to -1.7°C at the glacier-ocean interface at

292   ~260 m depth. For the Flade Isblink Ice Cap outlet, the cold glacier can significantly affect the water

293   column below the floating glacier tongue, generating a new water mass that can be colder than the

294   ambient PrW modified by interaction with the underlying warm AW. The sub-glacier freshwater discharge

295   can also reduce the salinity of this water mass; however, the sub-glacier discharge is likely negligible

296   during winter. For the floating glacier, a lateral interaction between the water below the glacier tongue and

297   the Atlantic-modified PrW can (i) give rise to the intrusions we observed at the base of the Halocline layer

298   and (ii) modify the background mixing line towards colder temperatures as also observed (Figures 6b and

299   7d). Similar intrusive interleavings at the front of a tidewater glacier were reported by *Jenkins* [1999],

300   *Mayer et al.* [2000] and *Stevens et al.* [2016].

301   For station SN15-13, located ~200 m from the termination of the tidewater glacier (Figure 4b), the

302   CTD profile shows an intrusion of cool, turbid water between 88 and 97 m depths that caused a temperature

303   inversion of -0.32°C and a sharp increase in the water turbidity from 0.2 to 1.5 NTU (Figure 8). A similar

304   rapid increase in turbidity with depth was also recorded at the Helheim Glacier in southeast Greenland

305   [*Straneo et al.*, 2011]. We attribute this increase to the lower boundary of the glacier tongue at 88 m depth.

306   In this case the turbid water can be attributed to subglacial discharge, or submarine melting of ice releasing

307   sediments. The currents (3-5 cm/s as a maximum, *Kirillov et al.*, 2017) are too weak for resuspending the

308   20 m thick bottom layer. Assuming the ratio of glacier/water densities to be 0.917, we get a glacier

309   elevation above the sea surface of ~7.5 m that corroborates with our visual estimates.

310   At the front of the glacier termination, the water below the depth of the glacier tongue is on average

311   cooler by 0.28°C and less salty (~0.2) than the ambient water as measured at SN15-09 (Cluster II; Figure

312   8), suggesting a lateral heat flux along with an insignificant sub-glacier fresh water discharge in winter

313   and/or a remnant of the larger discharge during summer. We suggest that interaction between the ambient

314   shelf water and water below the glacier tongue, modified in direct contact with glacier ice, deflects the

315   mixing line between the Halocline and AW in the *TS* space towards a lower temperature and, to a lesser

316   extent, to lower salinity values.

317   On the stations in cluster V, taken close to the tidewater glacier outlet, intrusions of colder, less

318   saline water are observed around 90 m depth, which is the estimated lower boundary of the floating ice

319   tongue. The water circulating below the glacier is initially warmer than the *in situ* freezing point of

320   seawater and will be cooled as it gets in contact with the bottom of the glacier. The lost heat is partly used

321   to melt ice and partly conducted into the glacier, increasing its temperature. Here we assume that the largest

322   part of the heat goes to melting and we presently ignore the fraction of heat conducted into the glacier. We

323   also ignore all other freshwater sources, e.g. runoff and seasonal ice melt, except that due to melting of the

324   glacier by ocean heat from below. The density reduction of the ocean water due to added melt water is

325   larger than the density increase due to cooling, and the less saline water will ascend along the lower

326   boundary of the glacier, until it terminus. At this point the water will penetrate into the ambient water

327   column at its density level few meters above the depth that the meltwater was released, forming colder, less

328   saline isopycnal intrusions.

329   To describe the interactions occurring below the floating glacier to the first order we then assume

330   that all heat lost by the water parcel is used to melt ice. The addition of meltwater leads to a salinity

331   reduction ΔS that can be estimated from:

332
$$\Delta S = \frac{S}{\left(\frac{L}{c_p \Delta T} - 1\right)}$$

333   Here c_p = 3980 J°C^{-1}kg^{-1} is the heat capacity of sea-water and L = 334500 Jkg^{-1} is the latent heat of melting.

334   ΔT is the temperature reduction and S is the salinity of the water parcel re-emerging from underneath the

335   glacier.

336   We do not have observations from below the floating glacier and we have to make assumptions

337   both about the initial characteristics of the water entering below the glacier and the cooling and reduction of

338   the salinity that occur by interaction with the glacier. The salinity of the water re-entering the water column

339   from below the glacier is $S \sim$ 33.65 and the observed temperature reduction, compared to the ambient

340   profiles, is $\Delta T \sim 0.3°C$ (Figures 4b and 6b). We know that the initial salinity then has to be higher than

341   33.65. Looking at the ambient profiles (Figure 5) we note that the mean temperature of the water that could

342   possibly enter beneath the glacier is about -0.8°C. Assuming it is cooled to freezing temperature, ΔT is 1°C

343   and ΔS becomes ~0.4. This gives an initial salinity of 34.05 to the water entering below the glacier.

344   However, the observed cold intrusions are not at the freezing point, instead they are warmer, around

345     $-1.4°C$ (Figure 8). This could indicate that the water entering below the glacier is not cooled to the freezing

346   point, but only by ~0.3°C. The initial salinity would then be 33.8 rather than 34.05. Another possibility is

347   that the cold water penetrates isopycnally into the water column and becomes warmer and more saline by

348   mixing with ambient water. Assuming that the intrusions are isopycnal, the changes in temperature and

349   salinity due to mixing becomes:

350
$$\alpha \Delta T = \beta \Delta S$$

351   Here $\alpha = 0.4 \times 10^{-4}$ °K^{-1} is the coefficient for the heat expansion around $-1°C$ and $\beta = 8 \times 10^{-4}$ psu^{-1} is the

352   coefficient of salt contraction. A temperature change of 0.5°C then corresponds to a salinity change of

353   0.025, making the salinity at the freezing point of 33.625, close to the observed 33.65 at the intrusion and

354   giving the initial salinity as 34.025. This suggests that the intrusions observed on the stations close to the

355   tidewater glacier outlet (Cluster V) might derive from the outflow of colder, less saline water created under

356   the floating ice tongue due to interactions between the glacier and the underlying water masses.

357

358   **4.2. Shelf water interaction with ambient water from the continental slope**

359   We use the occurrence of intrusive interleaving as a tracer for the shelf-slope interaction. The

360   intrusive Halocline from Cluster IV was observed to the north of Station Nord (Figure 4b) adjacent to the

361   Greenland continental slope, where a water mass with different thermohaline properties is located (Figure

362   5). The intrusions are indications of isopycnal interaction between the Atlantic-modified Halocline

363   occupied over the Wandel Sea shelf and a cooler PrW observed over the Wandel Sea continental slope

364   (Figure 5). Within the depth range of the Halocline (~65-100 m), the cooler PrW is likely maintained by

365   a weakened upward heat flux from the deepened AW in the off-shelf area. Over the Wandel Sea shelf, the

366   upper AW boundary was recorded at ~140 m, while in June-July 2015 and August 2008 it was ~30 m

367   deeper over the adjacent continental slope (Figure 5). We note, however, that the water mass structure over

368   the continental slope of Northeast Greenland shows significant interannual variability [e.g., *Falck et al.,*

369   2005]. Overall, the distinct difference between the on-shelf and off-shelf water mass structure (Figure 5)

370   suggests their different origins, which are further discussed in section 4.3.

371   In the following we speculate that the intrusive Halocline from Cluster IV is generated by

372   interaction between the Atlantic-modified shelf Halocline (Cluster II) and the PrW from the continental

373   slope as shown in Figure 9a. We suggest that this interaction is isopycnal because all intrusions are density

374   compensated. For the Halocline layer over the southern Wandel Sea continental slope, *Rudels et al.* [2005]

375   reported an intrusive interleaving conditioned by isopycnal interaction between relatively warm Halocline

376   water from the upper continental slope, and cold PrW from the lower continental slope.

377   For further interpretation of our results on the shelf-slope interaction we include 184 CTD profiles

378   taken between 1992 and 1993 in the NEW area [*Bignami and Hopkins*, 1997; *Budéus et al.*, 1997; *Falck,*

379   2001], which is downstream from the Wandel Sea shelf (Figures 1 and 2b). The *TS* curves from the NEW

380   area show two distinct modes: (i) the polynya (shelf) mode, which is similar to the "basic" Cluster II

381   derived for the Wandel Sea shelf (Figure 4b, 7a and dark blue lines in Figure 9a) except for a slightly

382   colder (~0.05°C) and saltier (~1) low Halostad, and (ii) the continental slope mode, which within the

383   salinity range of the Wandel Sea shelf Halocline (31.2-34) shows a completely different shape of the *TS*

384   curve (red lines in Figure 9a). Specifically the *TS* line of the continental slope mode extends linearly

385   through the Halostad to salinity of ~34 (red dashed line in Figure 9a; red rectangles in Figure 9b),

386   maintaining temperatures relatively close to the surface freezing temperature (blue dashed line Figure 9b).

387   For the NEW area, the remarkable difference between the polynya (shelf mode) and the continental

388   slope mode was also reported by *Straneo et al*. [2012] and *Wilson and Straneo* [2015], with a *TS* structure

389   similar to the one presented in Figure 9 (Figure 3 from *Wilson and Straneo*, 2015). Moreover, for the

390   79N glacier outlet (Figure 2b), *Straneo et al*. [2012] used the upper continental slope CTDs as ambient

391   stations and compared them to CTD profiles taken through a rift in the floating glacier tongue (see Figure

392   2b for the glacier station position). For the water layer at ~40-90 m depth, they reported ambient water that

393   was saltier than water below the glacier tongue by ~1-2, attributing this difference to the sub-glacier water

394   discharge. We note, however, that this freshening is of the same magnitude as the salinity difference

395   between the shelf Halostad/Halocline and the continental slope PrW (Figure 9). Thus, freshening reported

396   by *Straneo et al*. [2012] could be alternatively explained by the occurrence of the Halostad-like freshened

397   water layer below the glacier tongue.

398   In the following sections 4.3 and 4.4, we use the differences between the on-shelf and off-shelf

399   water mass structures and the similarities between the Wandel Sea and NEW areas to trace the origin of the

400   Halostad, Halocline and AW in the Wandel Sea and their modification along the northeast Greenland coast.

401

402   **4.3. Tracing the origin of the Wandel Sea Halostad, Halocline and AW: Local source**

403   The distinct difference between the on-shelf and off-shelf water mass structure and disposition

404   suggests they have different origins and/or pathways to the Wandel Sea shelf and continental slope. The

405   occurrence of the shelf Halostad can be explained by local freshening by summer snow/sea-ice melt water

406   and freshwater from the glacier runoff. In turn, the uplifted on-shelf Atlantic-modified PrW and AW can

407   originate from local modifications due to upwelling of AW over the Wandel Sea continental slope.

408   The under-ice surface layer over the Wandel Sea shelf is significantly freshened, potentially

409   providing a source of freshwater for the freshened Halostad over the shelf if vertical mixing overcomes the

410   salinity (density) stratified sub-surface halocline as was suggested for NEW by *Bignami and Hopkins*

411   [1997]. Among the Arctic shelves, the Wandel Sea sub-surface halocline shows exceptionally strong

412   vertical stratification with salinity increasing from 18 to 30 across a ~10 m thick sub-surface halocline layer

413   during winter (Figure 5). This is comparable to the Laptev Sea shelf where strong salinity stratification is

414 maintained by the river runoff from the Lena River, the second largest river flowing into the Arctic

415 Ocean [e.g., *Dmitrenko et al*., 2010]. *Dmitrenko et al*. [2012] showed that significant velocity shear over

416 the Laptev Sea shelf, attributed to the lunar semiduirnal baroclinic internal tide M2 with velocity ~15 cm/s

417 at 11 m and ~7 cm/s at 19 m depth is required to transform the vertically stratified water into a locally

418 mixed layer. In contrast, over the Wandel Sea shelf velocities hardly exceed 3-5 cm s^{-1}, and the most

419 energetic M2 tidal currents are weak, decreasing from ~2 cm/s beneath the ice to ~1 cm/s below 60 m depth

420 [*Kirillov et al.,* 2017]. Moreover, the multiyear landfast ice cover over the Wandel Sea shelf precludes the

421 wind stress from vertically mixing the stratified water column.

422   Hypothetically, the wind-driven upwelling of the Atlantic-modified PrW and AW over the

423 continental slope can result in uplift of the water masses over the outer shelf. In this case, however, the

424 shallowing of the Atlantic-modified PrW and the upper boundary of AW is accompanied by on-shelf

425 inflow of the deeper and saltier water from the continental slope. In contrast, the Atlantic-modified

426 Halocline on the shelf is less salty compared to ambient water from the continental slope by ~1-2.

427   In the following we discuss our results in the context of upstream observations in the Canada Basin

428 (e.g., Figure 10) and downstream observations in the NEW region.

429

430 **4.4. Tracing the origin of the Wandel Sea Halostad, Halocline and AW: Far field advection**

431   We suggest that the on-shelf Halostad and the associated Halocline can be advected from the remote

432 upstream areas where sources of fresh water exist. Similarly, as with the shelf Halostad, the shallowed AW

433 layer recorded over the Wandel Sea shelf and the deepened AW layer found over the continental slope

434 should be attributed to the different branches of the AW outflow from the Arctic Ocean through western

435 Fram Strait.

436   The East Greenland Current carries the Arctic Ocean outflow through western Fram Strait

437 southward along the Greenland shelf and continental slope – Figure 1 [e.g., *Rudels et al*., 2002; *Jeansson et*

438 *al*., 2008]. It transports cold, low salinity Polar surface waters with $\sigma_0 \leq 27.7$ kg m^{-3} [*Rudels et al*., 2002]

439   that are comprised of the river runoff and net precipitation water, but also of the less saline PcW that

440   enters the Arctic Ocean through Bering Strait [*Jones et al.*, 1998, 2003, 2008; *Rudels et al.*, 2002; *Falck et*

441   *al.*, 2005; *de Steur et al.*, 2009; *Sutherland et al.*, 2009] – Figure 1. PcW within the Arctic Ocean is

442   generally assigned to water with $S \leq 33$ [*von Appen and Pickart*, 2012] and has both a summer and winter

443   signature based on its formation. The summer PcW with temperatures above -1.2°C and salinities between

444   31 and 32 [*Steele et al.*, 2004] is usually comprised of the Chukchi Summer Water [*Woodgate et al.*, 2005]

445   and the Alaskan Coastal Water [*Pickart et al.*, 2005]. Below the summer PcW is a layer of winter PcW that

446   can be as cold as -1.45°C and forms during sea ice formation within the Bering and Chukchi Seas [*Jones*

447   *and Anderson*, 1986; *Weingartner et al.*, 1998; *Pickart et al.*, 2005].

448   It has been shown that the subsurface layer over the eastern Greenland coast is comprised of the

449   PcW outflow from the Arctic Ocean [*Jones et al.*, 1998, 2003, 2008; *Falck*, 2001; *Falck et al.*, 2005;

450   *Jeansson et al.*, 2008; *Sutherland et al.*, 2009]. For the 1993 observations over the NEW shelf area, in the

451   subsurface Halostad layer down to ~80 m depth, an average of about 90% is found to have Pacific origin

452   [*Falck*, 2001]. This result by *Falck* [2001] brought a different mechanism of the Halostad formation to

453   light. In contrast to *Bignami and Hopkins* [1997], *Falck* [2001] insists on an upstream Pacific source for the

454   Halostad water and underlying Halocline, rather than a local origin.

455   Upstream over the Canada Basin, PcW impacts the halocline structure, producing a double

456   halocline with a "cold Halostad" formed by the volumetric injection of the winter PcW that overlies Low

457   Halocline Water of the Eurasian Basin origin [*McLaughlin et al.*, 2004; *Shimada et al.*, 2005]. The salinity

458   range of the cold Halostad in the Canada Basin occupies $31.5 < S < 33.5$ with the lowest temperature of ~ -

459   1.7°C at the base of the Halostad indicating the winter PcW [*McLaughlin et al.*, 2004; *Shimada et al.*,

460   2005]. This water mass structure resembles that for the eastern Beaufort Sea continental slope (Figure 10).

461   In general, the Halostad structure over the Canada Basin and adjoining continental margin is similar

462   to that recorded over the Wandel Sea shelf (Figure 5). However, over the Wandel Sea shelf the Halostad is

463   cooler and fresher (Figure 10c) occupying a salinity range of $30.0 < S < 31.5$. The Wandel Sea Halostad is

464 also shallower (15-65 m depth versus ~50-200 for the Canada Basin). The different salinity range of the

465 Halostad in the Wandel Sea and Canada Basin suggests that significant modifications occurred during

466 transit of the winter PcW from the Bering and Chukchi Seas to the Wandel Sea. It seems that the winter

467 PcW is modified by vertical mixing with overlaying summer PcW and/or river runoff accumulated in the

468 Canada Basin. For example, *Jones et al.* [2008] revealed that over the northeast Greenland coast at ~81°N,

469 the PcW fraction is comparable with the river water fraction. Moreover, water from the Siberian shelves,

470 especially the Laptev Sea shelf also has the same salinity and temperature range and can mix into and cool

471 the summer PcW [e.g., *Dmitrenko et al.*, 2011]. This assumes that the river water impacts a Wandel Sea

472 Halostad initially comprised of the winter PcW.

473 The remote origin of the Halostad is also confirmed by the elevated values of the CDOM

474 fluorescence through the Halostad layer at station SN15-13 (Figure 8). The CDOM fluorescence is a good

475 tracer of the Arctic Ocean terrigenous organic matter primarily attributed to the Eurasian and American

476 continental runoff water [e.g., *Granskog et al.*, 2012] as well as to interactions with sediments on the Arctic

477 shelves [e.g., *Guéguen et al.*, 2007]. The CDOM fluorescence maxima in the Halostad at station SN15-13

478 is consistent with results from the Canada Basin where this maxima is attributed to the winter PcW [e.g.,

479 *Guéguen et al.*, 2007] and the continental river runoff water [e.g., *Granskog et al.*, 2012]. For the

480 downstream NEW area, *Amon et al.* [2003] also reported the intermediate maxima of the CDOM

481 fluorescence through the shelf Halostad layer (Figure 9a from *Amon et al.*, 2003). Overall, this confirms the

482 remote origin of the Halostad layer over the Wandel Sea shelf and strengthens our discussion on the

483 modification of the Pacific-derived Halostad by river runoff while en route from the Canada Basin to Fram

484 Strait.

485 As the Halocline and AW move along the Canada Basin margins toward northern Greenland, they

486 ascend in the water column from 100-200 m and 220-320 m in the Canada Basin [*McLaughlin et al.*, 2004;

487 *Shimada et al.*, 2005] to 85 m and 140 m on the Wandel Sea shelf, respectively (Figure 5). Following

488 *Rudels et al.* [2004], we speculate that this rise is due to the gradual thinning of the low salinity layer

489   above. The thinning could be caused by the upper layer either being confined to the Beaufort Gyre or

490   draining through the Canadian Arctic Archipelago and ultimately into Baffin Bay [*Rudels et al.*, 2004].

491   This is consistent with a gradual shallowing of the upper boundary of AW traced by isopycnal $\sigma_0 = 27.4$ kg

492   m^{-3} from ~230 m in the Canada Basin to ~140 m in the Wandel Sea [*Polyakov et al.*, 2010].

493   The occurrence of the Pacific origin Halostad along the northeast Greenland coast suggests that

494   PcW is transported southward by a narrow coastal branch of the East Greenland Current. This current also

495   advects a shallowed AW, which likely originated from the Canada Basin branch (Figure 1). The cross-slope

496   interaction between the coastal and off-shelf branches of the East Greenland Current gives rise to the

497   intrusive interleaving observed over the Wandel Sea outer shelf (Figure 7c).

498

5. Summary and conclusions

500   The first-ever CTD observations over the Wandel Sea shelf and continental slope were collected in

501   April-May and June-July 2015, respectively. We use CTD profiles deeper than 100 m to focus on the origin

502   of water masses, and to identify interactions between the shelf and slope, and between the ocean and outlet

503   glaciers entering the Wandel Sea. The stations taken on the Wandel Sea shelf and farther to the east on the

504   Greenland slope reveal two pathways for the advected water masses, one over the shelf and one along the

505   continental slope. The one over the slope has warm, saline AW lying below a deep, cold, less saline and

506   fairly homogenous upper layer that is capped by low salinity surface water created by seasonal ice melt and

507   heated by solar radiation. This suggests that AW recirculating within the Eurasian Basin (Figure 1) with the

508   less dense upper layer initially formed by sea ice melt water are mixed into the upper part of the entering

509   AW. In the Nansen Basin this layer is homogenized by haline convection each winter [*Rudels et al.*, 1996].

510   The water column found on the shelf has much colder and less saline AW located closer to the

511   surface than the AW over the slope. The AW characteristics here are similar to those observed at much

512   greater depth in the Canada Basin, indicating that this AW has circulated around the entire deep Arctic

513   basins and now is returning towards Fram Strait. In the Canada Basin, the AW is covered by the halocline

514 layer and it is comprised of both Atlantic ($S \sim 34$) and Pacific derived water, especially the Pacific

515 Winter Water, with $S \sim 33.1$ [e.g., *Jones and Anderson*, 1986], as well as other low salinity waters. These

516 low salinity waters lie shallower than the sill depth of the Canadian Arctic Archipelago and can pass

517 through the straits into Baffin Bay. This would cause the AW to rise in the water column as it moves along

518 the northern Canadian coast, until it is shallow enough to flow over deeper shelves like that of the Wandel

519 Sea.

520 Over the Wandel Sea shelf, the Pacific Winter Water, that was so distinct in the Canada Basin,

521 seems to be either missing or only occupying a narrow depth range. Instead the coldest water is found in

522 the Halostad with salinity around 31 instead of 33. The low salinity upper layer and the thick ice cover in

523 winter preclude the local homogenization of the water column down to the Halostad. Thus, the Halostad

524 must be advected from elsewhere. A conceivable scenario could be that most of the PcW drains out of the

525 Arctic Ocean through the Canadian Arctic Archipelago. This likely makes the AW ascend and it would

526 allow water from the Polar Mixed Layer, of Atlantic or Pacific origin, circulating in the Beaufort Gyre and

527 in the Arctic basins to replace the water leaving through the straits in the archipelago and penetrate onto the

528 shelf, creating a different upper layer above the AW.

529 Our findings are summarised as follows:

530 (i) The sub-surface (15-70 m depth) "cold Halostad" layer with salinities of 30-31.5 and associated

531 underlying Halocline layer is a distinct feature of the Wandel Sea shelf hydrography. It does not persist

532 over the Wandel Sea continental slope, indicating the water masses over the shelf and slope have different

533 origins. A similar water mass structure was observed downstream in the Northeast Water Polynya area.

534 This structure is likely maintained by the coastal branch of the Pacific Water outflow from the Arctic

535 Ocean, modified by interaction with river runoff water over the upstream Canada Basin.

536 (ii) The Halocline layer centered at ~ 80 m (salinity of ~ 33) separates the Pacific-origin cold

537 Halostad from the Polar Water, modified by interaction with warm Atlantic water outflow from the Arctic

538 Ocean through western Fram Strait. The upper boundary of the Atlantic Water ($T \sim 0°C$) is recorded at

539 ~170 m depth on the continental slope and ~30 m shallower over the adjoining shelf. This difference

540 suggests that, as with the subsurface layer, the intermediate water over the shelf and continental slope is

541 conditioned by different branches of the Atlantic water outflow from the Arctic Ocean.

542   (iii) The lateral shelf-slope interaction between on-shelf relatively warm Atlantic-modified

543 Halocline water and off-shelf cold Polar Water gives rise to the intrusive interleaving observed over the

544 Wandel Sea outer shelf.

545   (iv) At the base of the Halocline layer, cold and turbid water intrusions were recorded at the front of

546 the tidewater glacier outlet. The temperature-salinity plots of the CTD profiles from this region show a

547 mixing line that is deflected relative to the ambient water. Both features are likely conditioned by the

548 ocean-glacier thermal interaction.

549   In summary, our analysis suggests the existence of a coastal branch of the East Greenland Current

550 advecting Pacific Water of Arctic origin southward along the northeast Greenland coast. This is consistent

551 with an earlier proposition by *Rudels et al*. [2004], downstream observations along the southeast coast of

552 Greenland [e.g., *Bacon et al.,* 2002; *Sutherland and Pickart*, 2008; *Sutherland et al*. 2009] and numerical

553 simulations [*Hu and Myers*, 2013; *Aksenov et al*., 2016]. Finally, we note that our observations were not

554 accompanied by water sampling for determining the nitrate/phosphate relationship commonly used to trace

555 the Pacific Water in the Arctic Ocean and Greenland Sea. This deficiency in the observational program

556 conducted clearly shows the necessity for further research in this area using advanced methods of tracer

557 analysis.

558

559 **Acknowledgments:** This study was funded by the Canada Excellence Research Chair program (SR), the

560 Canada Research Chair program (DB), the Canada Foundation of Innovation, the National Sciences and

561 Engineering Research Council of Canada (grant RGPIN-2014-03606, ID), the Manitoba Research and

562 Innovation Fund, the University of Manitoba, Aarhus University, the Greenland Institute of Natural

563 Resources, and the EU project NACLIM (grant agreement 308299, BR). We thank Ivali Lennert, Kunuk

564 Lennert and Egon Frandsen for technical assistance in the field. We also appreciate outstanding logistical

565 support from the Station Nord Danish military personnel. John Mortensen (Greenland Climate Research

566 Centre) provided valuable comments on the ocean-glacier interaction. Comments and editing by Dr. John

567 K. Hall, the owner of the research hovercraft SABVABAA, are highly appreciated. Dr. Nils Nørgaard-

568 Pedersen kindly provided bathymetric data used in Figure 4a. This work is a contribution to the Arctic

569 Science Partnership (ASP) and the ArcticNet Networks of Centres of Excellence programs. For the Wandel

570 Sea CTD data contact ID at igor.dmitrenko@umanitoba.ca

571

572 **Reference**

573 Aksenov, Y., et al. (2016), Arctic pathways of Pacific Water: Arctic Ocean Model Intercomparison
574 experiments, *J. Geophys. Res. Oceans*, 121, 27–59, doi:10.1002/2015JC011299.

575 Amon, R. M. W., G. Bude´us, and B. Meon (2003), Dissolved organic carbon distribution and origin in the
576 Nordic Seas: Exchanges with the Arctic Ocean and the North Atlantic, *J. Geophys. Res*., 108(C7), 3221,
577 doi:10.1029/2002JC001594.

578 Bacon, S., G. Reverdin, I. G. Rigor, and H. M. Smith (2002), A freshwater jet on the east Greenland shelf,
579 *J. Geophys. Res*., 107(C7), 3068, doi:10.1029/2001JC000935.

580 Bendtsen, J., J. Mortensen, K. Lennert, J. K. Ehn, W. Boone, V. Galindo, Y. Hu, I. A. Dmitrenko, S. A.
581 Kirillov, K. K. Kjeldsen, Y. Kristoffersen, D. G. Barber, and S. Rysgaard (2017), Sea ice breakup and
582 marine melt of a retreating tidewater outlet glacier in northeast Greenland (81°N), *Sci. Rep*., 7, 4941, doi:
583 10.1038/s41598-017-05089-3.

584 Bignami, F. and T. S. Hopkins (1997), The water mass characteristics of the Northeast Water Polynya:
585 Polar Sea data 1992–1993, *J. Marine Sys.*, 10, 139-156.

586 Budéus, G., W. Schneider and G. Kattner (1997), Distribution and exchange of water masses in the
587 Northeast Water polynya (Greenland Sea), *J. Marine Sys.*, 10, 139-156.

588 de Steur, L., E. Hansen, R. Gerdes, M. Karcher, E. Fahrbach, and J. Holfort (2009), Freshwater fluxes in
589 the East Greenland Current: A decade of observations, *Geophys. Res. Lett*., 36, L23611,
590 doi:10.1029/2009GL041278.

591 Dmitrenko, I. A., S. A. Kirillov, T. Krumpen, M. Makhotin, E. P. Abrahamsen, S. Willmes, E. Bloshkinab,
592 J. A. Hölemann, H. Kassens and C. Wegner (2010), Wind-driven diversion of summer river runoff
593 preconditions the Laptev Sea coastal polynya hydrography: Evidence from summer-to-winter hydrographic
594 records of 2007–2009, *Continental Shelf Research*, 30(15), 1656-1664, doi:10.1016/j.csr.2010.06.012.

595 Dmitrenko, I. A., V. V. Ivanov, S. A. Kirillov, E. L. Vinogradova, S. Torres-Valdes, and D. Bauch (2011),
596 Properties of the Atlantic derived halocline waters over the Laptev Sea continental margin: Evidence from
597 2002 to 2009, *J. Geophys. Res*., 116, C10024, doi:10.1029/2011JC007269.

Dmitrenko, I. A., S. A. Kirillov, E. Bloshkina, and Y.-D. Lenn (2012), Tide-induced vertical mixing in the Laptev Sea coastal polynya, *J. Geophys. Res.*, 117, C00G14, doi:10.1029/2011JC006966.

Dmitrenko, I. A., S. A. Kirillov, A. Forest, Y. Gratton, D. L. Volkov, W. J. Williams, J. V. Lukovich, C. Belanger, and D. G. Barber (2016), Shelfbreak current over the Canadian Beaufort Sea continental slope: Wind-driven events in January 2005, *J. Geophys. Res. Oceans*, 121, 2447–2468, doi:10.1002/2015JC011514.

Eicken, H. (1994), Structure of under-ice melt ponds in the central Arctic and their effect on the sea-ice cover, *Limnol. Oceanogr.*, 39(3), 682-694.

Falck, E. (2001), Contribution of waters of Atlantic and Pacific origin in the Northeast Water Polynya, *Polar Res.*, 20(2), 193–200.

Falck, E., G. Kattner, and G. Bude´us (2005), Disappearance of Pacific Water in the northwestern Fram Strait, *Geophys. Res. Lett.*, 32, L14619, doi:10.1029/2005GL023400.

Flocco, D., D. L. Feltham, E. Bailey, and D. Schroeder (2015), The refreezing of melt ponds on Arctic sea ice, *J. Geophys. Res.*, 120, 647-659, doi:10.1002/2014JC010140.

Granskog, M. A., C. A. Stedmon, P. A. Dodd, R. M. W. Amon, A. K. Pavlov, L. de Steur, and E. Hansen (2012), Characteristics of colored dissolved organic matter (CDOM) in the Arctic outflow in the Fram Strait: Assessing the changes and fate of terrigenous CDOM in the Arctic Ocean, *J. Geophys. Res.*, 117, C12021, doi:10.1029/2012JC008075.

Guéguen, C., L. Guo, M. Yamamoto-Kawai, and N. Tanaka (2007), Colored dissolved organic matter dynamics across the shelf-basin interface in the western Arctic Ocean, *J. Geophys. Res.*, 112, C05038, doi:10.1029/2006JC003584.

Hu, X. and P. G. Myers (2013), A Lagrangian view of Pacific water inflow pathways in the Arctic Ocean during model spin-up, *Ocean Modelling*, 71, 66–80, doi:10.1016/j.ocemod.2013.06.007.

Inall, M. E., T. Murray, F. R. Cottier, K. Scharrer, T. J. Boyd, K. J. Heywood and S. L. Bevan (2014), Oceanic heat delivery via Kangerdlugssuaq Fjord to the south-east Greenland ice sheet, *J. Geophys. Res.*, 119, 631-645, doi: 10.1002/2013JC009295.

Jeansson, E., S. Jutterström, B. Rudels, L. G. Anderson, K. A. Olsson, E. P. Jones, W. M. Smethie Jr. and J. H. Swift (2008), Sources to the East Greenland Current and its contribution to the Denmark Strait Overflow, *Progress in Oceanography*, 78, 12-28, doi: 10.1016/j.pocean.2007.08.031

Jenkins, A. (1999), The impact of melting ice on ocean waters, *J. Phys. Oceanogr.*, 29(9), 2370-2381.

Jones, E. P. and L. G. Anderson (1986), On the origin of the chemical properties of the Arctic Ocean halocline, *J. Geophys. Res.*, 91, C9, 10,759-10,767, doi: 10.1029/JC091iC09p10759.

Jones, E. P., L. G. Anderson, and J. H. Swift (1998), Distribution of Atlantic and Pacific waters in the upper Arctic Ocean: Implications for circulation, *Geophys. Res. Lett.*, 25, 765-768.

Jones, E. P., J. H. Swift, L. G. Anderson, M. Lipizer, G. Civitarese, K. K. Falkner, G. Kattner and F. A. McLaughlin (2003), Tracing Pacific water in the North Atlantic Ocean, *J. Geophys. Res.*, 108(C4), 3116, doi: 10.1029/2001JC001141.

635 Jones, E. P., L. G. Anderson, S. Jutterström and J. H. Swift (2008), Sources and distribution of fresh
636 water in the East Greenland Current, *Progress in Oceanography*, 78, 37–44,
637 doi:10.1016/j.pocean.2007.06.003.

638 Kattner, G. (2009), The Expedition of the Research Vessel "Polarstern" to the Arctic in 2008 (ARK-
639 XXIII/2), *Berichte zur Polarforschung*, 590, 88 p.

640 Kirillov, S., I. Dmitrenko, S. Rysgaard, D. Babb, L. T. Pedersen, J. Ehn, J. Bendtsen, and D. Barber (2017),
641 Storm-induced water dynamics and thermohaline structure at the tidewater Flade Isblink Glacier outlet to
642 the Wandel Sea (NE Greenland), *Ocean Sci. Discuss*., doi: 10.5194/os-2017-60.

643 McLaughlin, F. A., E. C. Carmack, R. W. MacDonald, H. Melling, J. H. Swift, P. A. Wheeler, B. F. Sherr
644 and E. B. Sherr (2004), The joint roles of Pacific and Atlantic-origin waters in the Canada Basin, 1997–
645 1998, *Deep Sea Res. Part I*, *51*, 107–128.

646 Mayer, C., N. Reeh, F. Jung-Rothenhausler, P. Huybrechts, and H. Oerter (2000), The subglacial cavity and
647 implied dynamics under Nioghalvfjerdsfjorden Glacier, NE-Greenland, *Geophys. Res. Lett*., 27(15), 2289–
648 2292.

649 Nørgaard-Pedersen, N., N. Mikkelsen and Y. Kristoffersen (2008), Late glacial and Holocene marine
650 records from the Independence Fjord and Wandel Sea regions, North Greenland, *Polar Res*., 27, 209-221,
651 doi:10.1111/j.1751-8369.2008.00065.x.

652 Palmer, S. J., A. Shepherd, A. Sundal, E. Rinne, and P. Nienow (2010), InSAR observations of ice
653 elevation and velocity fluctuations at the Flade Isblink ice cap, eastern North Greenland, *J. Geophys. Res*.,
654 115, F04037, doi:10.1029/2010JF001686.

655 Pickart, R.S., T. J. Weingartner, L. J. Pratt, S. Zimmermann and D. J. Torres (2005), Flow of winter-
656 transformed Pacific water into the western Arctic, *Deep-Sea Res*. II, 52, 3175–3198.

657 Polyakov, I. V., L. A. Timokhov, V. A. Alexeev, S. Bacon, I. A. Dmitrenko, L. Fortier, I. E. Frolov, J.-C.
658 Gascard, E. Hansen, V. V. Ivanov, S. Laxon, C. Mauritzen, D. Perovich, K. Shimada, H. L. Simmons, V. T.
659 Sokolov, M. Steele and J. Toole (2010), Arctic Ocean warming contributes to reduced polar ice cap, *J.*
660 *Physical Oceanography*, 40(12), 2743-2756, doi: 10.1175/2010JPO4339.1.

661 Rinne, E. J., A. Shepherd, S. Palmer, M. R. van den Broeke, A. Muir, J. Ettema, and D. Wingham (2011),
662 On the recent elevation changes at the Flade Isblink Ice Cap, northern Greenland, *J. Geophys. Res*., 116,
663 F03024, doi:10.1029/2011JF001972.

664 Rudels, B., E. P. Jones, L. G. Anderson, and G. Kattner (1994), On the intermediate depth waters of the
665 Arctic Ocean, In: *The Polar Oceans and Their Role in Shaping the Global Environment: The Nansen*
666 *Centennial Volume, Geophys. Monogr. Ser.,* vol. 849 85, Johannessen, O. M., R. D. Muench, and J. E.
667 Overland (Eds.), pp. 33-46, AGU, Washington, D. C.

668 Rudels, B., L. G. Anderson, and E. P. Jones (1996), Formation and evolution of the surface mixed layer and
669 halocline of the Arctic Ocean, *J. Geophys. Res*., 101(C4), 8807–8821, doi:10.1029/96JC00143.,.

670 Rudels, B., E. Fahrbach, J. Meincke, G. Budéus and P. Eriksson (2002), The East Greenland Current and its
671 contribution to the Denmark Strait overflow, *ICES Journal of Marine Science*, 59, 1133–1154,
672 doi:10.1006/jmsc.2002.128.

Rudels, B., E. P. Jones, U. Schauer and P. Erikssondels (2004), Atlantic sources of the Arctic Ocean surface and halocline waters, *Polar Res.*, 23(2), 181–208.

Rudels, B., G. Björk, J. Nilsson, P. Winsor, I. Lake and C. Nohr (2005), The interaction between waters from the Arctic Ocean and the Nordic Seas north of Fram Strait and along the East Greenland Current: results from the Arctic Ocean-02 Oden expedition, *Journal of Marine Systems*, 55, 1–30, doi:10.1016/j.jmarsys.2004.06.008.

Rudels, B. (2012), Arctic Ocean circulation and variability – advection and external forcing encounter constraints and local processes, *Ocean Sci.*, 8, 261–286, doi:10.5194/os-8-261-2012.

Shimada, K., M. Itoh, S. Nishino, F. McLaughlin, E. Carmack, and A. Proshutinsky (2005), Halocline structure in the Canada Basin of the Arctic Ocean, *Geophys. Res. Lett.*, 32, L03605, doi:10.1029/2004GL021358.

Steele, M., J. Morison, W. Ermold, I. Rigor, M. Ortmeyer, and K. Shimada (2004), Circulation of summer Pacific halocline water in the Arctic Ocean, *J. Geophys. Res.*, 109, C02027, doi:10.1029/2003JC002009.

Straneo, F., R. G. Curry, D. A. Sutherland, G. S. Hamilton, C. Cenedese, K. Våge and L. A. Stearns (2011), Impact of fjord dynamics and glacial runoff on the circulation near Helheim Glacier, *Nature Geoscience*, 4, 322–327, doi:10.1038/ngeo1109.

Straneo, F., D. Sutherland, D. Holland, C. Gladish, G. S. Hamilton, H. L. Johnson, E. R. Ringot, Y. Xu and M. Koppes (2012), Characteristics of ocean waters reaching Greenland's glaciers, *Annals of Glaciology*, 53(60), 202-210, doi: 10.3189/2012AoG60A059.

Stevens, L. A., F. Straneo, S. B. Das, A. J. Plueddemann, A. L. Kukulya and M. Morlighem (2016), Linking glacially modified waters to catchment-scale subglacial discharge using autonomous underwater vehicle observations, *Cryosphere*, 10, 417–432, doi: 10.5194/tc-10-417-2016.

Sutherland, D. A., and R. S. Pickart (2008), The East Greenland Coastal Current: Structure, variability, and forcing, *Prog. Oceanogr.*, 78(1), 58-77, doi:10.1016/j.pocean.2007.09.006.

Sutherland, D. A., R. S. Pickart, E. Peter Jones, K. Azetsu-Scott, A. Jane Eert, and J. Ólafsson (2009), Freshwater composition of the waters off southeast Greenland and their link to the Arctic Ocean, *J. Geophys. Res.*, 114, C05020, doi:10.1029/2008JC004808.

Sutherland, D. A. and F. Straneo (2012), Estimating ocean heat transports and submarine melt rates in Sermilik Fjord, Greenland, using lowered acoustic Doppler current profiler (LADCP) velocity profiles, *Ann. Glaciology*, 53, 50–58, doi:10.3189/2012AoG60A050.

von Appen, W.-J. and R. S. Pickart (2012), Two Configurations of the Western Arctic Shelfbreak Current in Summer, *J. Phys. Oceanogr.* 42, 329-351, doi: 10.1175/JPO-D-11-026.1.

Walsh, D. and E. Carmack (2003), The nested structure of Arctic thermohaline intrusions, *Ocean Modelling*, 5(3), 267–289, doi:10.1016/S1463-5003(02)00056-2.

Weingartner, T., D. Cavalieri, K. Aagaard, and Y. Sasaki (1998), Circulation, dense water formation, and outflow on the northeast Chukchi shelf, *J. Geophys. Res.*, 103 (C4), 7647-7661.

Wexler, H. (1960), Heating and melting of floating ice shelves, *J. Glaciology*, 3, 626-645.

710 Wilson, N. J., and F. Straneo (2015), Water exchange between the continental shelf and the cavity
711 beneath Nioghalvfjerdsbræ (79 North Glacier), *Geophys. Res. Lett.*, 42, 7648–7654,
712 doi:10.1002/2015GL064944.

713 Woodgate, R. A., K. Aagaard, and T. J. Weingartner (2005), A year in the physical oceanography of the
714 Chukchi Sea: Moored measurements from autumn 1990-1991, *Deep-Sea Res. Part II*, 52 (24-26), 3116-
715 3149, doi: 10.1016/j.dsr2.2005.10.016.

716 Woodgate, R. A., K. Aagaard, J. H. Swift, W. M. Smethie Jr., and K. K. Falkner (2007), Atlantic water
717 circulation over the Mendeleev Ridge and Chukchi Borderland from thermohaline intrusions and water
718 mass properties, *J. Geophys. Res.*, 112, C02005, doi:10.1029/2005JC003416.

719 Woodgate, R. (2013), Arctic Ocean Circulation: Going Around At the Top Of the World, *Nature Education*
720 *Knowledge*, 4(8), 8.

721 **Tables**

722 **Table 1**: The Wandel Sea water mass structure below 15 m depth

Water layer	Acronym	Property range			
		Depth, m	Temperature, °C	Salinity	σ_0, kg m^{-3}
Halostad (of Pacific origin)	-	~ 15÷65	~ -1.5 ÷ -1.75	30÷31.2	24.1÷25.1
Pacific Water	PcW	PcW comprises the Halostad			
Halocline	-	~ 65÷100	~ -1.75 ÷ -0.65	31.2÷34	25.1÷27.3
Atlantic-modified Polar Water	PrW	~100÷140	-1.15 ÷ 0	34÷34.5	27.3÷27.7
Atlantic Water	AW	>140	>0 (up to 0.3)	>34.5	>27.7

723

724 **Table 2**: Description of the Wandel Sea CTD clusters

Cluster #	Cluster name	Station #	Main features	Property range			
				Depth m	Temp. °C	Salinity	σ_0 kg m^{-3}
I	Open water	31, 35, 53, 54, 79-83	"Warm" Halostad	15÷65	~ -1.6	30.0÷31.2	24.2÷25
			Smooth TS curves	>65	-1.7÷-0.8	>31.2	>25
II	Basic	8-11, 66, 68	"Cold" Halostad	15÷65	-1.6÷-1.72	30.0÷31.2	24.2÷ 25
			Smooth TS curves	>65	-1.7÷-0.8	>31.2	>25
III	Transit	6, 7, 58, 59, 67, 71	Moderate intrusions with temperature anomalies < 1 standard deviation	65-90	-1.25÷-1.6	31.2÷ 33.5	25.6÷ 26.7
IV	Intrusive	62-65, 69, 70	Significant intrusions with negative temperature anomalies > 1 standard deviation	65-90	-1.25÷-1.7	31.2÷ 33.5	25.3÷26.7
V	Glacier	13, 73, 73, 75	Significant intrusions	90-100	-1.2÷-1.4	33.5÷33.85	>27.1
			Deflected mixing line	>100	>-1.2	>33.85	>27.2

725

726

727   **Figures**

728

729

730

731

732
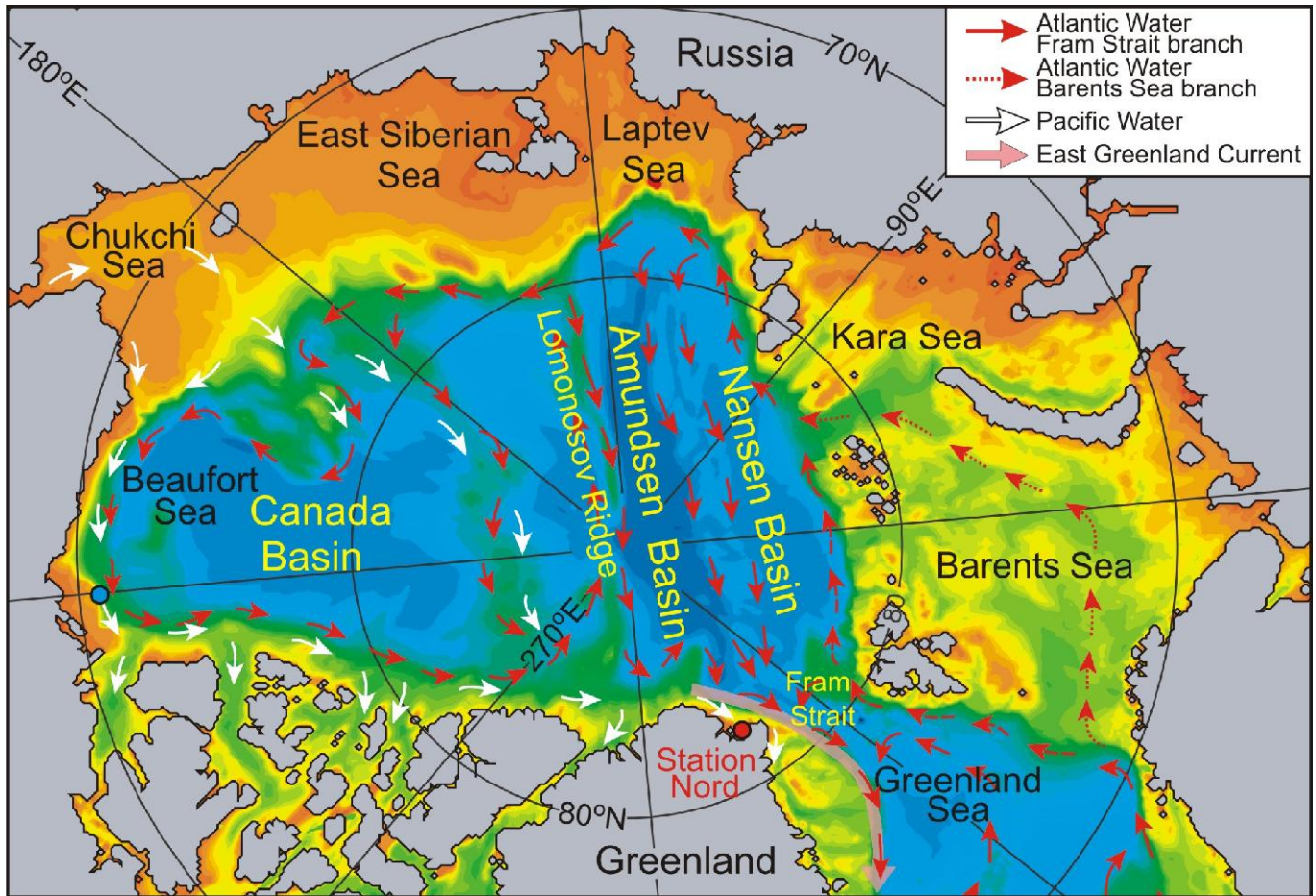
733   **Figure 1:** Schematic circulation of the Atlantic Water (AW, red arrows) and Pacific Water (PcW, white
734   arrows) in the Arctic Ocean and adjoining Greenland Sea following *Rudels et al.* [1994], *Jones* [2001],
735   *Rudels* [2012], and *Woodgate* [2013]. The dashed and dotted red arrows correspond to the Fram Strait and
736   Barents Sea branches of the AW inflow, respectively. The pink arrow indicates the East Greenland Current.
737   The red dot depicts the position of Station Nord in Northeast Greenland. The blue dot roughly identifies
738   location where CTD profiles were collected in the Beaufort Sea.

739
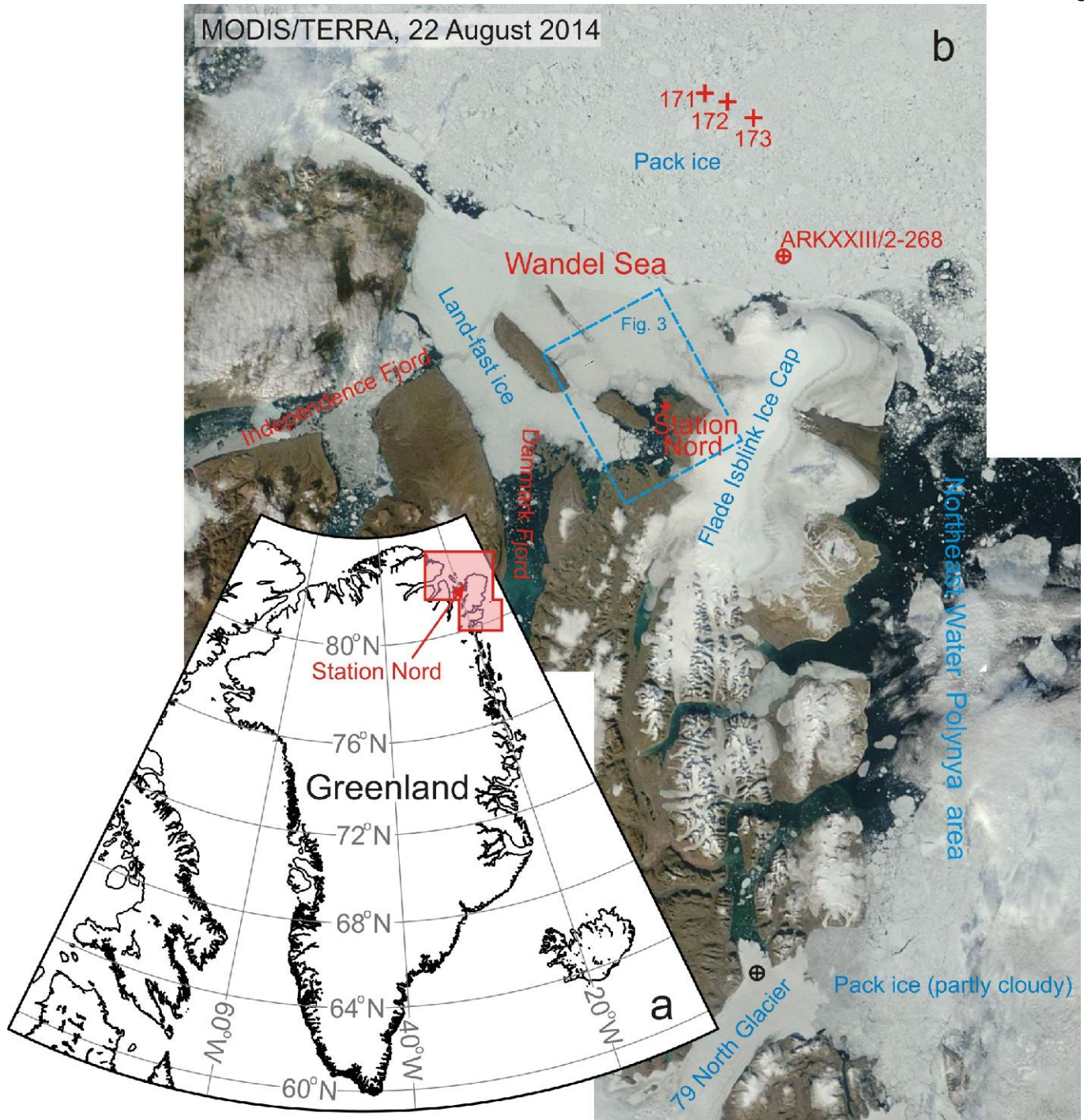
Figure 2: (**a**) Station Nord (SN) on the Greenland map. The pink shading highlights the Wandel Sea region with adjoining fjord system, Flade Isblink Ice Cap (FIIC), the Northeast Water Polynya (NEW) area and the 79 North Glacier outlet enlarged in panel (**b**). (**b**) The MODIS/TERRA satellite image from 22 August 2014 taken over the SN/FIIC/NEW area. Red and black circled crosses indicate the CTD stations occupied over the Wandel Sea outer-shelf during the ARKXXIII/2 expedition in August 2008 and in a rift in the 79 North Glacier in August 2009. Red crosses depict the CTD stations occupied in June-July 2015 over the Wandel Sea continental slope (> 1000 m depth) during the Norwegian FRAM 2014-15 sea ice drift. The dashed blue rectangle indicates the 2015 study area shown in Figure 3.

749

750
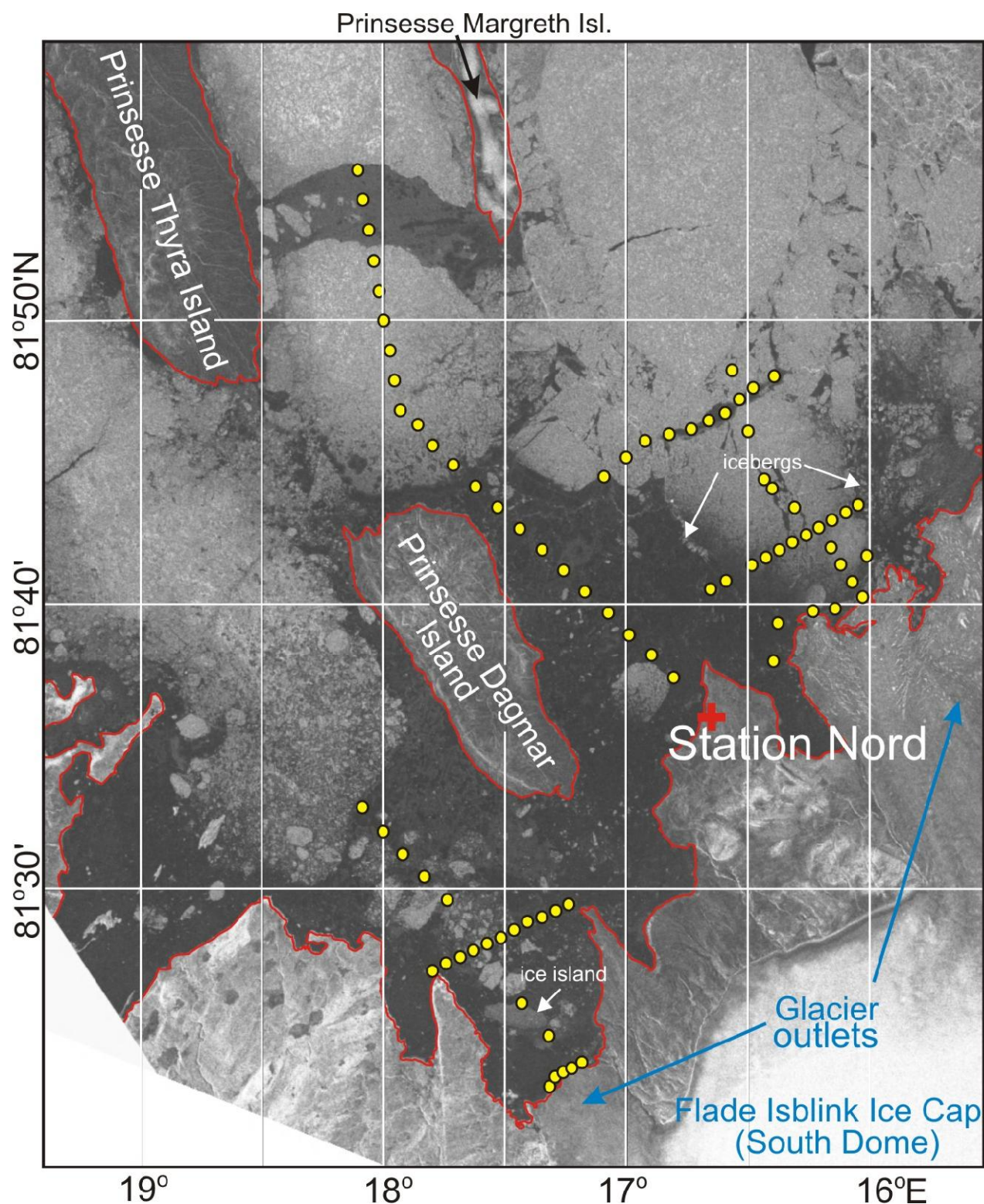
Figure 3: The Sentinel-1 C-SAR image from 2 February 2015 with the CTD stations overlaid. The dark areas along the coast are associated with first year landfast ice (< 1.8 m thick). The lighter areas indicate the multi-year landfast ice (~2 m to > 4 m thick). Yellow circles identify stations with CTD measurements Blue arrows indicate the northern outlet glaciers of the Flade Isblink Ice Cap.

755

756

757

758

759

760
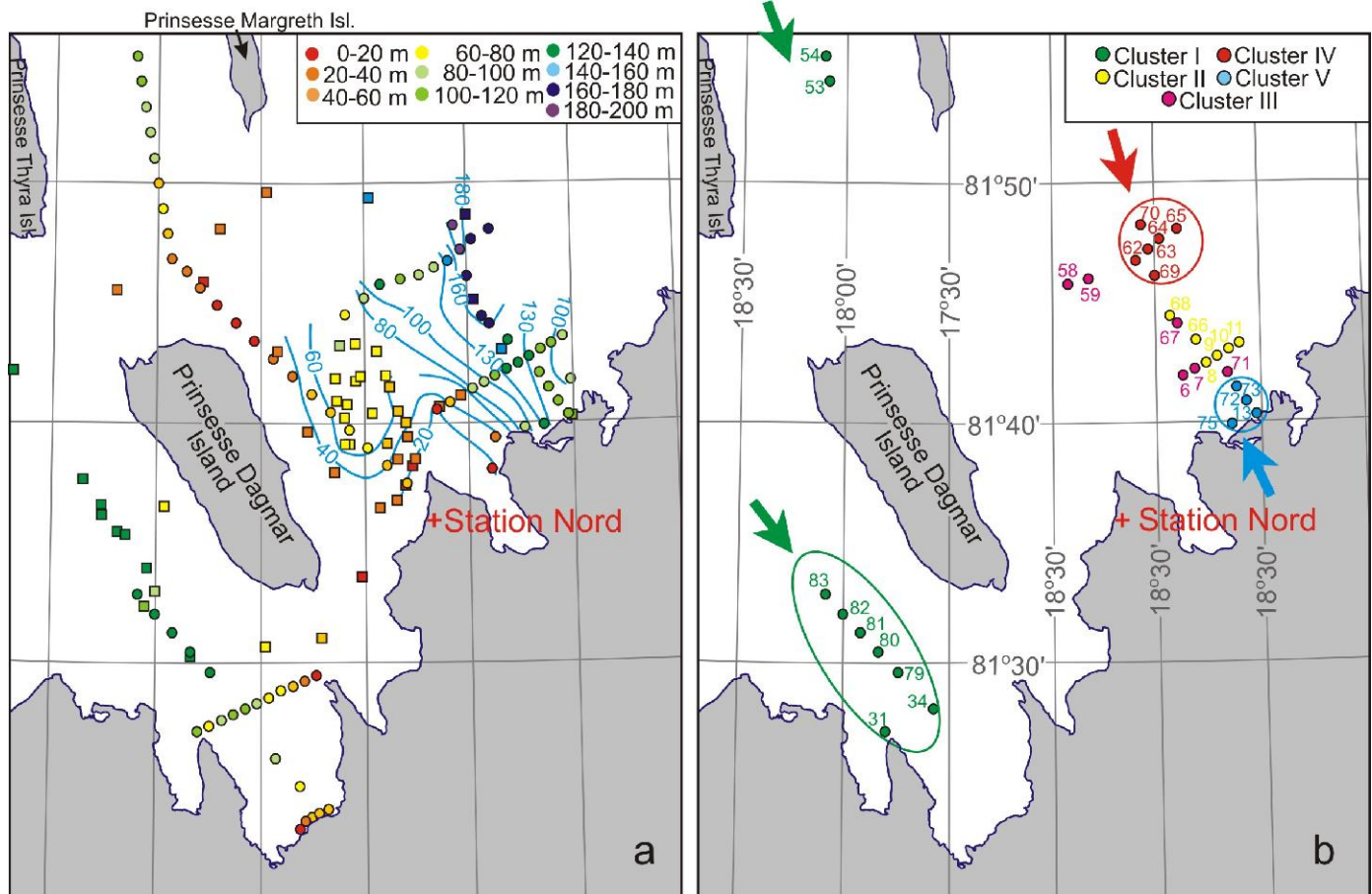
Figure 4: CTD stations occupied in April-May 2015 (circles). (**a**) Depth shown by color and blue contour lines. In addition, rectangles identify stations with depth measured in May 2006 (adopted from *Nørgaard-Pedersen et al.*, 2008) and April 2015. (**b**) CTD stations > 100 m depth are grouped in clusters derived from the *TS* analysis. They are identified by their station numbers. Arrows depict deep water pathways.
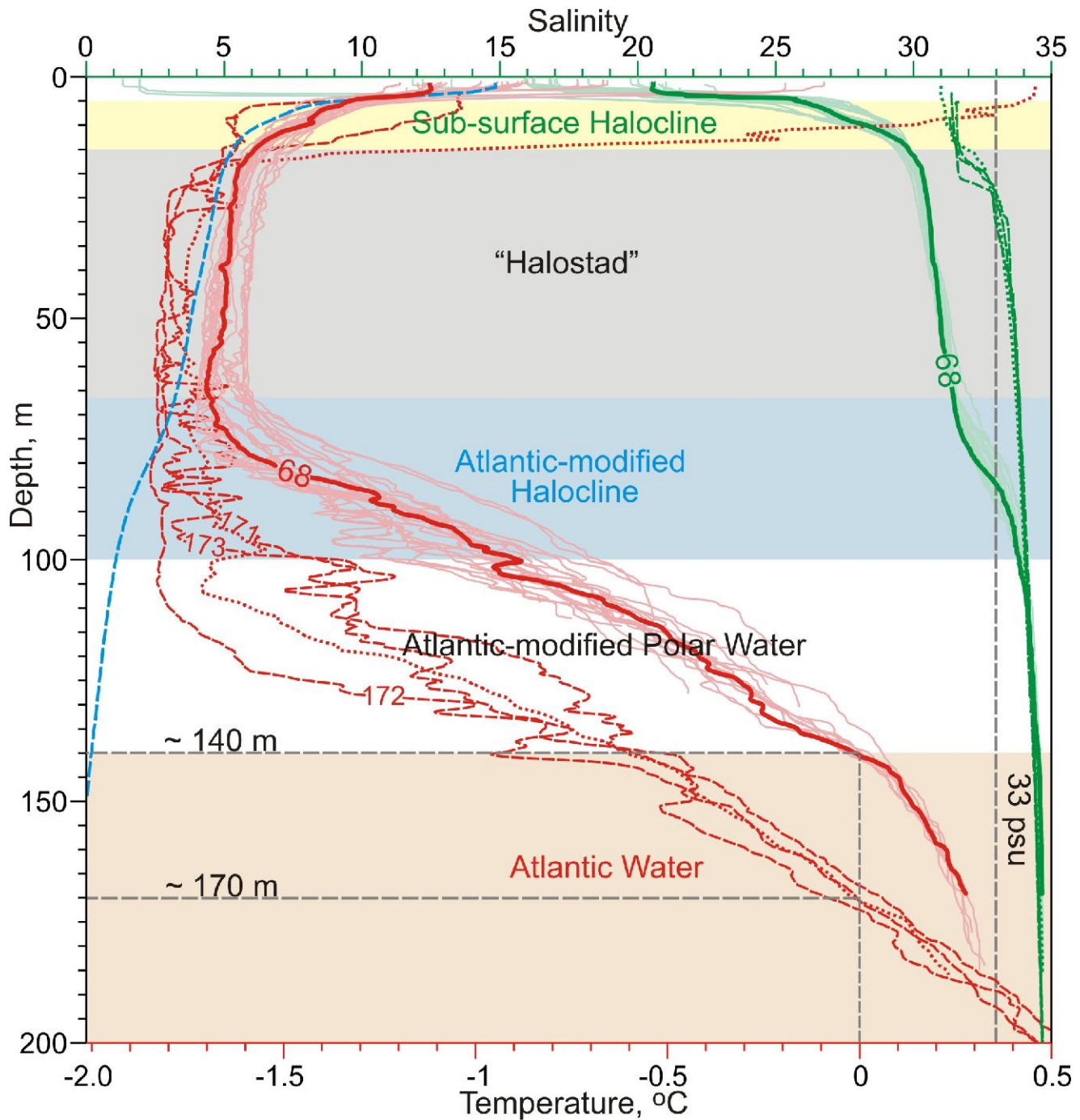
Figure 5: Vertical distribution of temperature (red) and salinity (green) profiles over the Wandel Sea shelf (≥ 100 m depth; solid curves) from April and May 2015, over the continental slope (stations 171-173; dashed curves) from June and July 2015 from the Norwegian FRAM 2014-15 ice drift (see Figure 2b for station position) and on the Wandel Sea upper continental slope (ARKXXIII/2 268; dotted curves) from RV Polarstern on 2 August 2008 [*Kattner,* 2009]. Thick red and green lines show typical vertical profiles of salinity and temperature, respectively, for station STN15-68. The blue dashed curve is the *in situ* temperature of freezing computed using the mean SN salinity profile (not shown). The vertical dashed line depicts salinity of 33 that separates the PcW and AW in the western Beaufort Sea [*von Appen and Pickart,* 2012].
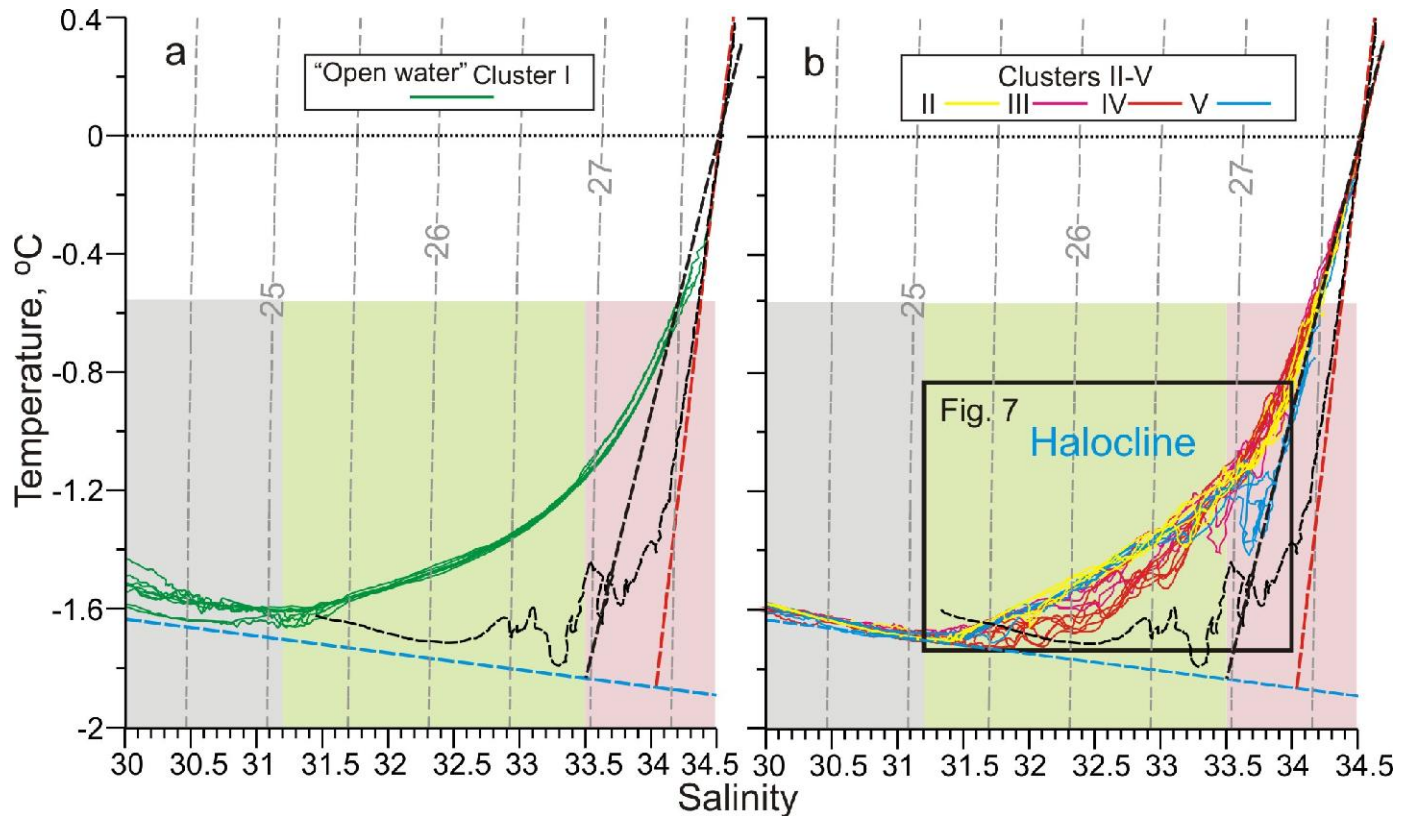
Figure 6: *In situ* temperature and salinity curves for the CTD stations >100 m depth with σ_0 isopycnals presented (dashed grey lines; kg m^{-3}). (**a**) CTD profiles grouped into Cluster I "Open Water". (**b**) CTD profiles grouped into Clusters II–V. The halocline layer of the water column is enlarged in Figure 7 where Clusters II-V are distinguished. We also present an approximation of thermohaline properties for the downstream Atlantic-modified PrW over the NEW continental slope (dashed red line; adopted from *Falck*, 2001) and the profile from Station 172 over the Wandel Sea continental slope (thin black dashed line). The surface freezing temperature is also presented (dashed blue line). An approximation of the meltwater mixing line from interaction with the glacial tongue is derived from Cluster V by fitting the data in *TS* space (thick black dashed line). The panels are shaded according to the corresponding water masses; gray represents the Halostad, while green and pink represent the halocline and define the salinity used for clustering.

795

796

797

798

799

800

801
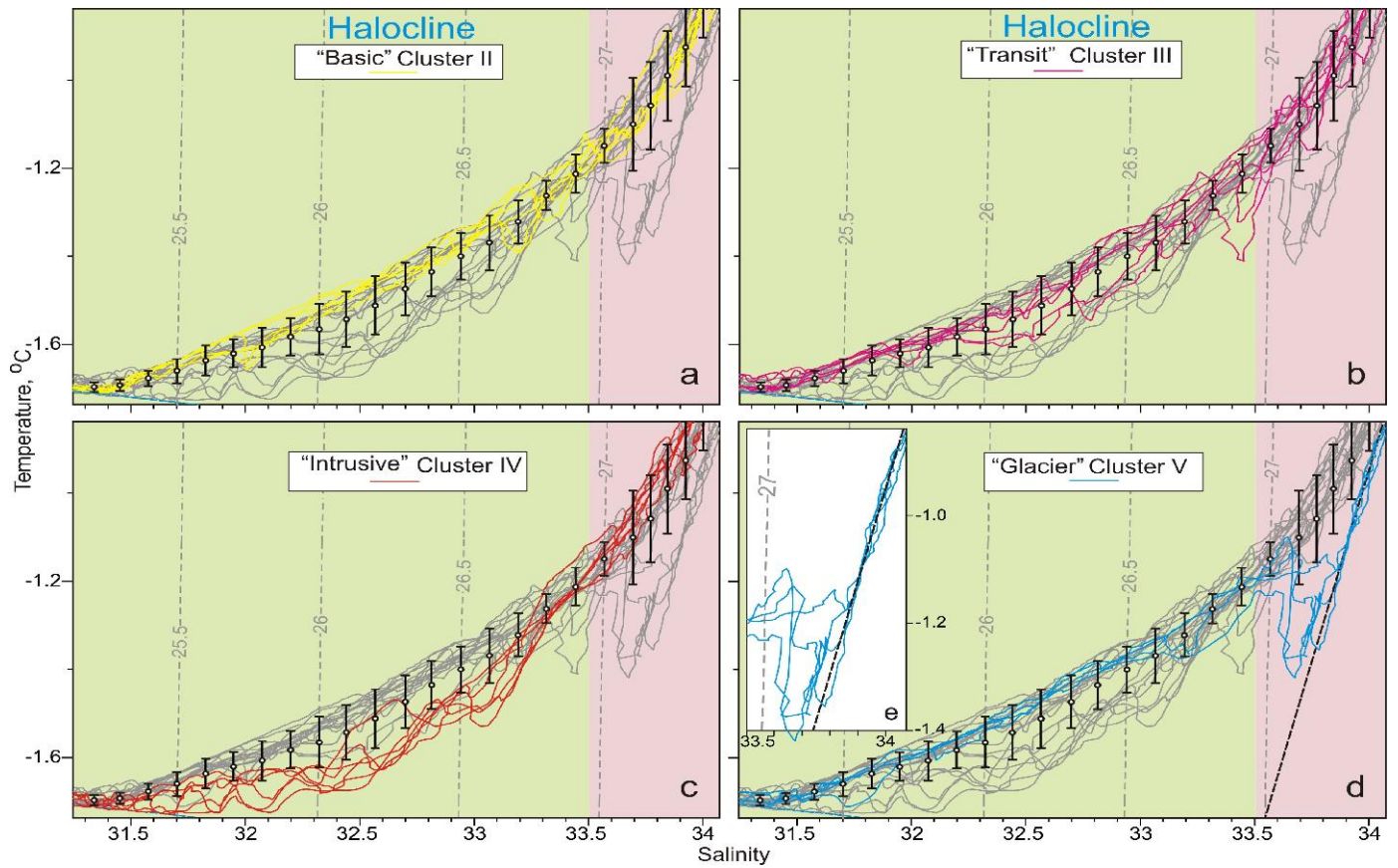
Figure 7: In situ temperature and salinity curves for the CTD profiles grouped into Clusters (**a**) II (yellow), (**b**) III (purple), (**c**) IV (red) and (**d**) V (blue) overlaid over the profiles from other clusters (grey) . The mean TS characteristics ±1 standard deviation (white barred dots) are presented at isopycnal intervals of 0.1 kg m^{-3}. All other designations are similar to those in Figure 6. (**e**) Temperature and salinity curves below the glacier depth for the CTD profiles grouped into Cluster V.

807

808

809

810

811

812

813

814
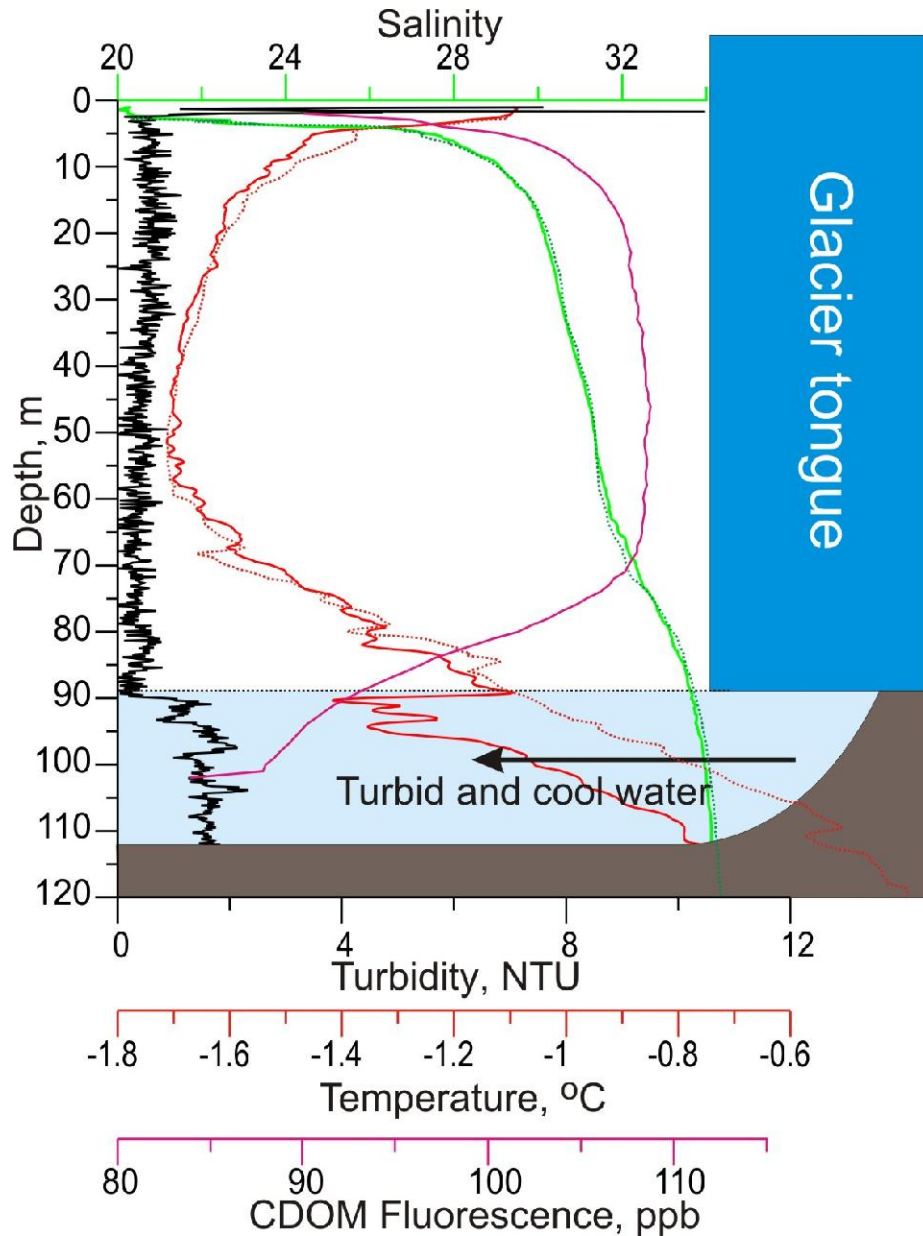
Figure 8: Vertical distribution of temperature (°C, red), salinity (green) and turbidity (NTU, black) at station SN15-13 (Cluster V; solid lines) in front of the tidewater glacier. The CDOM fluorescence (ppb) from the moored ITP WETLabs Optical sensor shown for the 21 April – 11 May mean (solid violet line) for the same location. An ambient profile from SN15-09 (Cluster II; dotted lines) is presented for comparison. The black dotted line at ~90 m depth indicates the suggested depth of the glacier tongue. The glacier tongue is depicted schematically

822

823
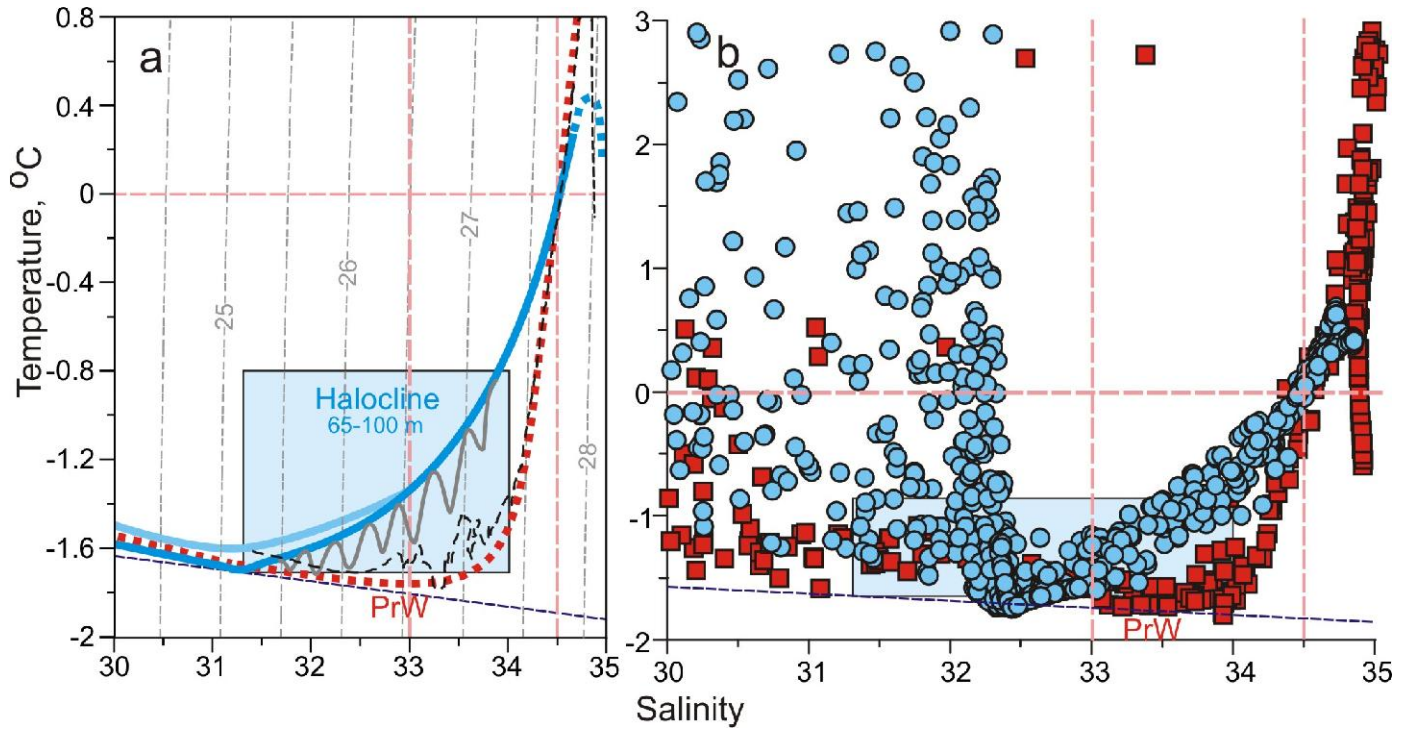
Figure 9: (**a**) Schematic showing formation of the intrusive halocline in clusters III and IV due to interleaving between the PcW (blue curve) and PrW (red dotted curve). Gray curve depicts the intrusive activity. The black dashed curve is station 172 from the Wandel Sea continental slope. The dashed red curve is approximation of the downstream PrW and AW properties at the Greenland continental slope, the NEW area adopted from (**b**). The solid dark/light blue curves are approximations of the PcW and upper AW from Clusters I/II. The dashed blue curve is approximation of the AW properties over the Greenland shelf in the NEW area adopted from (**b**). The gray dashed lines are σ_0 isopycnals in kg m^{-3}. (**b**) Temperature and salinity curves for the CTD stations taken in July-August 1993 between 76.5°N and 81°N and west of 5° W over the NEW area after *Falck* [2001]. Blue circles depict stations from the polynya (shelf) area. Red rectangular depict stations from the Greenland continental slope and Belgica Trough. (**a, b**) Blue shading highlights the approximate properties of the Wandel Sea shelf halocline. The dashed dark blue line is surface freezing temperature.

841

842

843

844

845

846

847

Figure 10: (**a**) Temperature (°C) and (**b**) salinity distributions across the Beaufort Sea continental slope
compiled based on 201 ArcticNet CTD profiles occupied between the 225°E and 226°E from June to
October 2002-2011 (adopted from *Dmitrenko et al*., 2016). (**c**) In situ mean temperature and salinity curves
for the cross-slope Beaufort Sea section (red) and the Wandel Sea shelf CTD profiles from the "basic"
Cluster II (black). Shading depicts ±1 standard deviation. The red and black dotted rectangles indicate
thermohaline properties of the Halostad over the Beaufort Sea continental slope and Wandel Sea shelf,
respectively. The dashed blue line is surface freezing temperature. The gray dashed lines are σ_0 isopycnals
in kg m^{-3}.